












# Gold and Silver Nanoparticles Efficiently Modulate the Crosstalk Between Macrophages and Cancer Cells

Dóra Izabella Adamecz <sup>1,2</sup>, Éva Veres <sup>2-4</sup>, Csaba Papp <sup>3,4</sup>, Hédi Árva <sup>1,2</sup>, Andrea Rónavári <sup>5</sup>, Annamária Marton <sup>6</sup>, Csaba Vizler <sup>6</sup>, Attila Gácsér <sup>3,4</sup>, Zoltán Kónya <sup>5</sup>, Nóra Igaz <sup>1,\*</sup>, Mónika Kiricsi <sup>1,\*</sup>

<sup>1</sup>Department of Biochemistry and Molecular Biology, University of Szeged, Szeged, Hungary; <sup>2</sup>Doctoral School of Biology, University of Szeged, Szeged, Hungary; <sup>3</sup>Department of Biotechnology and Microbiology, University of Szeged, Szeged, Hungary; <sup>4</sup>HCEMM-SZTE Pathogen Fungi Research Group, University of Szeged, Szeged, Hungary; <sup>5</sup>Department of Applied and Environmental Chemistry, University of Szeged, Szeged, Hungary; <sup>6</sup>Laboratory of Tumor Immunology and Pharmacology, Centre of Excellence of the European Union, HUN-REN Biological Research Centre, Szeged, Hungary

\*These authors contributed equally to this work

Correspondence: Mónika Kiricsi; Nóra Igaz, Department of Biochemistry and Molecular Biology, University of Szeged, Közép fasor 52, Szeged, H-6726, Hungary, Email kiricsim@gmail.com, kiricsim@bio.u-szeged.hu; nora.igaz@bio.u-szeged.hu, noraigaz@gmail.com

**Background:** Macrophages, polarized into pro-inflammatory M1 or anti-inflammatory M2 states, are essential cellular elements of innate immunity. In the tumor microenvironment, owing to a paracrine manipulative program by cancerous cells, tumor-associated macrophages (TAMs) evolve, which can shift between M1-like and M2-like phenotypes. Since it is fairly unknown how the promising anticancer agents, silver (AgNPs) and gold nanoparticles (AuNPs) affect the bidirectional communication and reprogramming in the tumor stroma, we examined the behavior, the tumor-supporting functions, and the expression of polarization and functional marker genes of TAMs to reveal how these are modulated upon interaction with nanoparticle-exposed cancer cells.

**Methods:** We established co-cultures of murine immortalized J774 or primary bone marrow-derived macrophages with 4T1 breast cancer cells treated with AuNPs or AgNPs or with none of the nanoparticles. We assessed the expression of macrophage polarization and functional markers using RT-qPCR and Proteome Profiler Array and evaluated macrophage migration and matrix metalloproteinase activity by specific assays.

**Results:** Protein and mRNA levels of most examined factors – except tumor necrosis factor- $\alpha$  – such as C-C-motif chemokine ligands 2 and 22, interleukin-23, inducible nitric oxide synthase, cyclooxygenase-2, the macrophage mannose receptor CD206, transforming growth factor- $\beta$ , and chitinase-like-3 protein decreased, and the expression of polarization markers revealed a shift towards M1-like phenotype in macrophages co-cultured with AgNP- or AuNP-treated 4T1 cells. Both nanoparticle treatments reduced the levels and activity of cell migration-related factors, such as C-C motif chemokine ligand 3, matrix metalloproteinases, and suppressed macrophage migration.

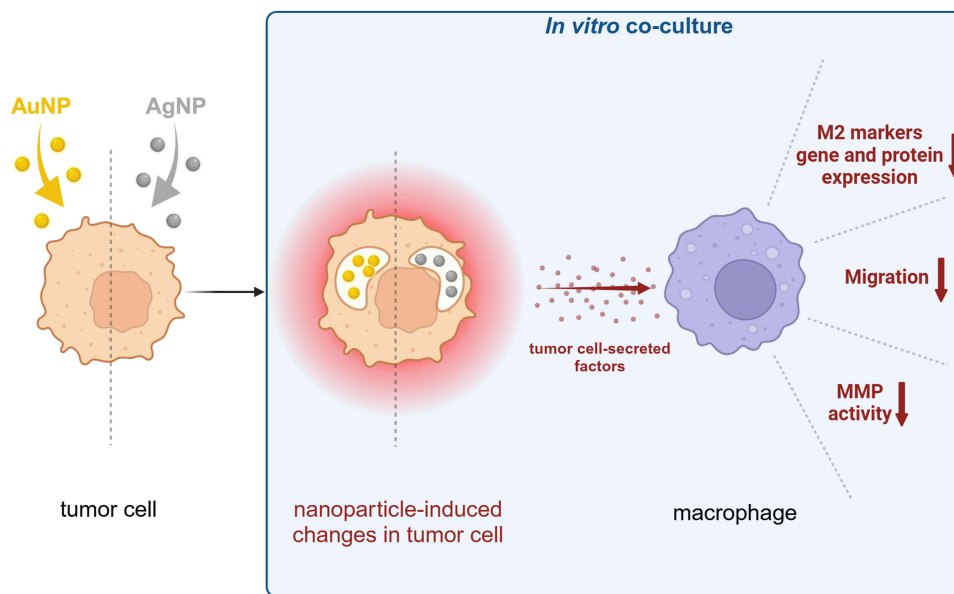
**Conclusion:** Both AuNPs and AgNPs showed a remarkable ability to influence macrophage-cancer cell communication, suppressed indirectly M2-like TAM polarization, and perturbed the migration behavior of TAMs that is critical for tumor invasion, indicating modulated immunological functions and debilitated cancer-promoting capabilities of TAMs in this microenvironment.

**Keywords:** metal nanoparticles, tumor microenvironment, tumor-associated macrophage, macrophage-tumor cell co-culture, paracrine

## Introduction

Macrophages, crucial cellular components of innate immunity, exhibit high plasticity and a remarkable ability to differentiate in response to numerous stimuli; as a consequence, macrophages show extreme heterogeneity under both physiological and pathological conditions. These highly versatile effector immune cells respond to various environmental signals by undergoing polarization into different functional states or phenotypes. Generally, macrophage polarization can

## Graphical Abstract



result in M1, often called classically activated macrophages, or in M2, also known as alternatively activated macrophages.<sup>1–3</sup> M1 and M2 macrophages usually differ in their cell surface marker and secreted cytokine profiles, which ultimately determine their specific biological functions. M1 cells are primarily involved in pro-inflammatory responses and are activated upon exposure to pathogens, microbial products, and certain cytokines and chemokines; they themselves produce high levels of pro-inflammatory cytokines and efficiently kill pathogens. In contrast, M2 macrophages are activated by anti-inflammatory cytokines and are mainly involved in anti-inflammatory and tissue-repair functions such as wound healing.<sup>4</sup> Importantly, macrophage polarization is a highly dynamic process where cells can switch between these states in response to changing conditions.<sup>3</sup> Therefore, a broad spectrum of activation states between M1 and M2 phenotypes can evolve.

Tumor cells induce profound molecular, cellular, and physical alterations in their imminent surroundings, leading to the formation of a specific tumor microenvironment (TME), a continuously evolving, complex milieu dominated by tumor-induced interactions. Although the precise cellular composition of the TME can vary markedly across different tumor types, it always includes, next to cancer cells, a variety of non-cancerous stromal cells. Already in the early phases of tumor development, a reciprocal and dynamic relationship forms between cancer cells and other cellular components of the TME, facilitating cancer cell survival and proliferation, local invasion, and often metastatic dissemination.

Among others, macrophages are also active cellular components of the TME.<sup>5</sup> These cells, also known as tumor-associated macrophages (TAMs), originate from tissue-resident macrophages and bone marrow-derived monocytes.<sup>6,7</sup> Due to intricate cell-to-cell interaction networks and cellular reprogramming in the TME, similarly to other innate immune cells, macrophages often lose their ability to exercise antitumor effector functions and become co-opted to promote tumor growth.<sup>8</sup> Thus, TAMs can exhibit antitumoral or tumor-promoting phenotypes depending on their *in situ* stimuli-induced polarization; however, TAMs rarely display a clear M1 or M2 phenotype, therefore, the complexity of these cells cannot easily be resolved with the binary classification.<sup>9–11</sup> The M1-like and the M2-like TAMs represent the two endpoints of a continuous dynamic TAM polarization axis, each possessing unique cell surface markers and functional factors, therefore playing markedly different roles within the TME.<sup>12</sup> Several reports indicate that M1-TAMs are prevalent in the early stages of carcinogenesis and are capable of releasing inflammatory substances leading to inhibition of tumor growth.<sup>4</sup> However, chronic inflammation resulting from M1-like activity

might accelerate genomic instability in malignant cells and serve as a driver of tumor progression.<sup>13,14</sup> M1-like TAMs, besides promoting inflammation in the TME, inhibit cell proliferation, eliminate pathogens, and manifest antitumor responses. They secrete an extensive number of pro-inflammatory biomarkers, including tumor necrosis factor- $\alpha$  (TNF- $\alpha$ ) and interleukin-23 (IL-23), and generate chemokines like C-C motif chemokine ligand 2 (CCL2) and C-C motif chemokine ligand 3 (CCL3).<sup>2,12</sup> M1-like cells also release inducible nitric oxide synthase (iNOS or NOS2), reactive oxygen species, and several matrix-metalloproteinases (MMPs).<sup>12</sup> In the intermediate and later stages of tumorigenesis, the M2 phenotype takes over.<sup>4,15</sup> These cells are involved in anti-inflammatory activities, promoting angiogenesis, influencing tissue regeneration, and fostering tumor generation, proliferation, metastasis, and drug resistance. They express the macrophage mannose receptor (MMR or CD206) and chemokines like C-C motif chemokine ligand 2 (CCL2),<sup>12</sup> produce large amounts of MMPs, including MMP2 and MMP9, and release numerous anti-inflammatory factors, including transforming growth factor- $\beta$  (TGF- $\beta$ ), albeit expressing some pro-inflammatory proteins (eg CCL2, CCL3, IL-23) as well.<sup>16–19</sup> Among the distinguished M2-like TAM markers, we can also find cyclooxygenase-2 (COX2)<sup>20,21</sup> and chitinase-like 3 protein (Chil3 or Ym1),<sup>22</sup> that are overexpressed in the TME and correlate with poor prognosis in some types of cancer.

Numerous studies suggested that pharmacological modification of the continuous and mutual information exchange between stromal cells, such as TAMs, and tumor cells can hinder metastasis, enhance the efficiency of anticancer treatment, and ameliorate survival, further highlighting the supportive function of stromal cells upon tumor progression and metastatic dissemination.<sup>23–26</sup>

Nano-sized materials represent promising alternatives to small-molecule anticancer drugs in novel therapeutic modalities.<sup>27</sup> Owing to the unique physicochemical and biological properties, the simple synthesis, and versatile surface chemistry, the potential of metal nanoparticles in medicine is exponentially increasing.<sup>28</sup> Various studies on in vivo and in vitro cancer models have already shown that metal nanoparticles made of silver (AgNPs), gold (AuNPs), copper, platinum, or titanium, only naming a few, can efficiently attenuate tumor growth primarily by triggering apoptotic pathways in cancer cells.<sup>23,29–34</sup> AgNPs exhibit an intrinsic anticancer activity, as following their uptake into cancer cells, the release of reactive ions and generation of a massive amount of free radicals lead to inhibition of proliferation and induction of programmed cell death, often referred to as a “Trojan-horse” type mechanism.<sup>33,35,36</sup> AuNPs are considered as inert, biocompatible nanomaterials, since their easily modifiable surfaces are excellent platforms for targeted drug delivery.<sup>37,38</sup> These outstanding features of nanoparticles should be exploited in cancer therapy; however, caution should be taken as nanoparticles might induce undesired immune responses, causing inflammation and toxicity in non-target organs upon in vivo administration. The immune responses triggered by nanoparticles, their biodistribution, and potential toxic effect on the immune (eg spleen, liver, lymph nodes) or other organs (eg brain, lung) seem to depend strongly on the physicochemical characteristics of the applied nanomaterials; therefore, by selecting the appropriate size, charge, and stabilizing agents of the particles, these issues can be eliminated, and the involved immune components potentially modulated.<sup>39–44</sup>

In our previous study, we found that AuNPs and AgNPs modify the tumor-promoting activity of tumor-associated fibroblasts (CAFs),<sup>23</sup> so the focus of our attention turned to another abundant cell type in the TME, ie to TAMs. It was reported by others that direct exposure of macrophages to metal nanoparticles triggered the secretion of TNF- $\alpha$ , IL-1 $\beta$ , IL-6, iNOS, NF- $\kappa$ B, and IL-8.<sup>45–50</sup> Regarding specifically the tumor-associated types of macrophages, both nanoparticles reduced the secretion of TNF- $\alpha$ , IL-10, and increased the expression of IL-12 in TAMs, furthermore, AuNPs repressed the expression of TGF- $\beta$  and IL-10 and downregulated the proportion of CD163+ M2 macrophages. These results indicated that AgNPs and AuNPs are able to perturb the polarization and the immunological functions of TAMs.<sup>51,52</sup>

Although the impact of AgNPs and AuNPs on various cancer and some stromal cells has already been investigated, all these studies – also the ones detailed above – involved direct exposure of cells to particles and focused on the direct effects of metal nanoparticles on macrophages. Therefore, it is fairly unknown how such nanoparticles would affect the bidirectional cell communication and reprogramming in the tumor stroma and whether the presence of nanoparticles would influence the capacity of cancer cells to manipulate other cell types, such as TAMs, in their vicinity. Therefore, the present study was undertaken with the aim of examining the behavior, the tumor-supporting functions, and the expression

of various polarization and functional marker genes in TAMs to reveal how these are modulated upon interaction and exposure to cancer cells that were treated with metal nanoparticles.

## Material and Methods

### Synthesis and Characterization of Gold (AuNPs) and Silver Nanoparticles (AgNPs)

Quasi-spherical citrate-coated gold (AuNPs), as well as silver nanoparticles (AgNPs), were synthesized according to the modified Lee–Meisel method.<sup>53</sup> All chemicals for the nanoparticle synthesis were obtained from Merck (Darmstadt, Germany). Silver nitrate or tetrachloroauric acid was reduced by sodium borohydride in the presence of sodium citrate. In a typical synthesis, 20 mL of 1% w/v citrate solution and 75 mL of water were added to a beaker and heated to 70 °C. Then, 2 mL of 1% w/v silver nitrate solution was introduced into the mixture, followed by a drop-wise addition of 2 mL of 0.1% w/v freshly prepared sodium borohydride solution. The reaction solution was kept at 70 °C under vigorous stirring for 1 h and was then cooled to room temperature. The same procedure was followed with tetrachloroauric acid instead of silver nitrate for gold nanoparticle synthesis.

### Cell Cultures

Murine J774.2, hereinafter referred to as J774, macrophage-like (Sigma-Aldrich, St. Louis, MO, USA) and 4T1 mammary carcinoma cell lines (American Type Culture Collection, Manassas, VA, USA) were maintained in 4.5 g/L glucose Dulbecco's modified Eagle's medium (DMEM) supplemented with 10% heat-inactivated fetal bovine serum (FBS), 2 mm L-glutamine, 0.01% streptomycin and 0.005% ampicillin.

Culture of primary bone marrow-derived macrophages (BMDMs) was established from the bone marrows of 8- to 10-week-old female BALB/c mice in BMDM medium (80% [v/v] DMEM supplemented with 10% heat-inactivated FBS and 1% penicillin–streptomycin mixture; 20% [v/v] L929-conditioned medium) for 7 days in 6-well plates (around  $2 \times 10^6$  progenitor cells were seeded/well), according to the experiment ([Supplementary Material Figure S1A](#)).<sup>54,55</sup> Fresh medium was added every other day.

The L929 fibroblast murine cell line (Merck, Darmstadt, Germany), which produces macrophage colony-stimulating factor (M-CSF), was used to generate an L929-conditioned medium to facilitate macrophage differentiation. Confluent L929 cultures were incubated with unsupplemented 4.5 g/L glucose DMEM in 75 cm<sup>3</sup> tissue culture flasks for 10 days. The resulting cell culture supernatants were sterile-filtered, aliquoted, and stored at –80°C until use.

The functionality of the primary macrophage culturing method was validated using immunostaining with anti-CD11b and anti-F4/80 antibodies (BioLegend, San Diego, CA, USA) or isotype controls (BioLegend, San Diego, CA, USA), followed by flow cytometric analysis. Macrophages were identified as CD11b+ F4/80+ double-positive cells, which accounted for over 80% of the total population across all genotypes, confirming the effectiveness of the method. The successful differentiation of macrophages was checked by immunostaining with anti-CD11b and anti-F4/80 antibodies (BioLegend, San Diego, CA, USA) ([Supplementary Material Figure S1A](#) and [B](#)).<sup>56</sup>

### Cell Viability Assay

To determine the direct effect of AuNPs and AgNPs on the viability of 4T1 and J774 cells, a 3-(4,5-dimethylthiazol-2-yl)-2,5-diphenyltetrazolium bromide (MTT) assay was performed. For this,  $5 \times 10^3$  cells/well were seeded into 96-well plates (Biologix, Jinan, Shandong, China) and left to grow. On the next day, the samples were washed with phosphate-buffered saline (PBS), and the cells were treated with increasing concentrations of AuNPs (10, 20, 40, 60, 86, 172, 258, 344, 430 μM) or AgNPs (10, 20, 40, 80, 139, 278, 417, 556, 695 μM) diluted in cell culture medium containing 10% FBS. After 24 hours, treatments were removed, cells were washed with PBS, and 0.5 mg/mL MTT reagent diluted in DMEM medium was added to the cells for an hour. Formazan crystals were dissolved in dimethylsulfoxide (DMSO, Serva Electrophoresis GmbH, Heidelberg, Germany), and the absorbance of the samples was measured at 570 nm by Synergy HTX plate reader (BioTek, Biotek Instruments Inc., Winooski, VT, USA). Experiments were repeated three times using three independent biological replicates. Experiments were performed using at least three independent biological replicates.



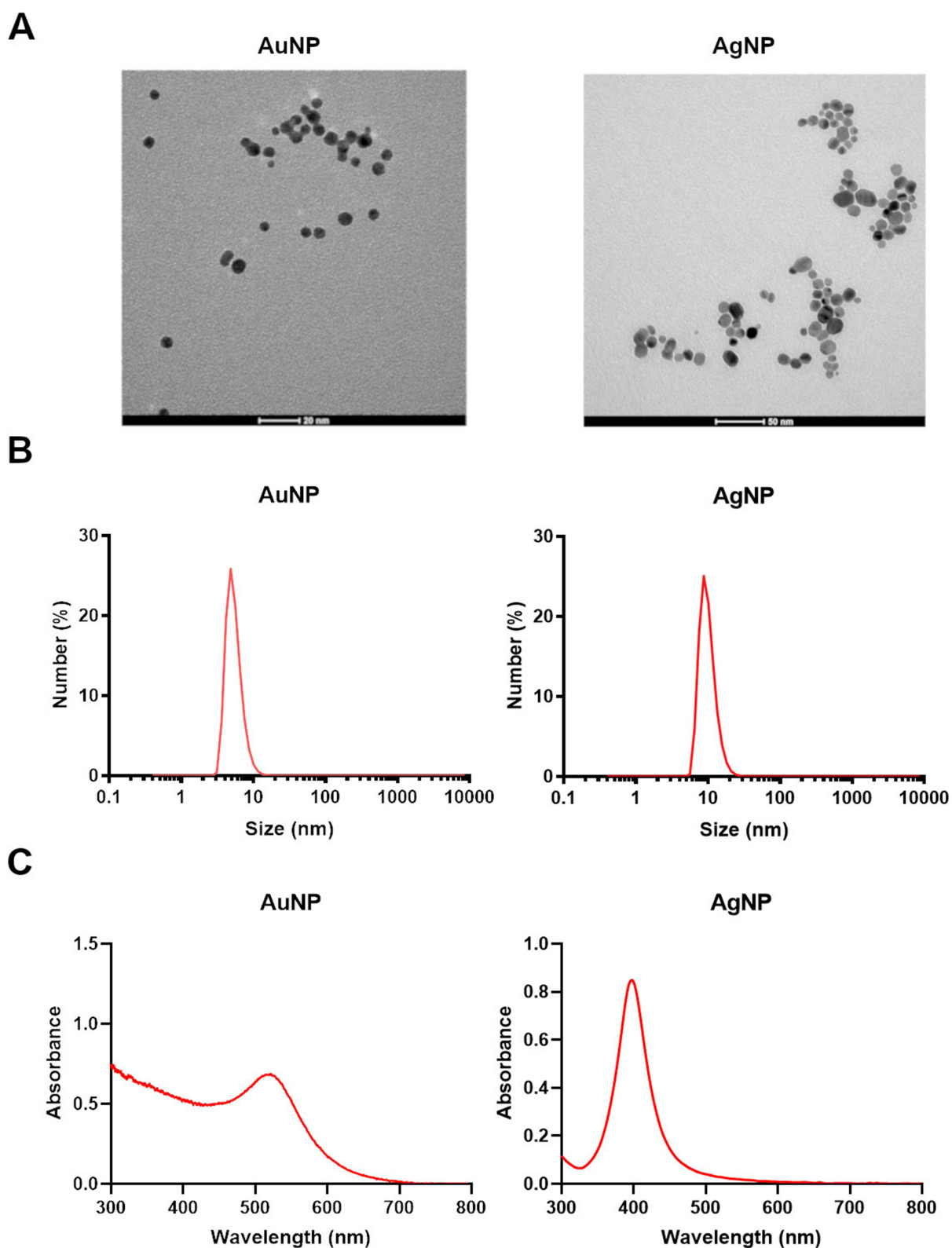


**Figure 1** Physicochemical characterization of the synthesized gold (AuNPs) and silver (AgNPs) nanoparticles. **(A)** Representative transmission electron microscopic images of AuNPs and AgNPs, **(B)** size distribution by dynamic light scattering of metal nanoparticles, and **(C)** ultraviolet-visible spectra obtained of AuNPs and AgNP samples.

## Electron Microscopy

The uptake of AuNPs and AgNPs by 4T1 cancer cells and J774 macrophages was verified by transmission electron microscopy (TEM). For this,  $10^5$  cells were seeded onto 0.4  $\mu\text{m}$  pore size polyester membrane inserts (Corning, NY, USA), and on the following day, the cultures were incubated with 40  $\mu\text{M}$  of AuNPs or 20  $\mu\text{M}$  of AgNPs for 24 h. Then, cells were washed with PBS and fixed in 4% glutaraldehyde. Samples were first embedded in gelatin, then sliced into 1–2 mm cubes, and embedded in epoxy (Embed 812, EMS, PA 19440). To identify the cell monolayer, semi-thin sections of 1  $\mu\text{m}$  were prepared, and thin sections of 70 nm were obtained and stained with uranyl and lead solutions. Images were captured by a Jeol JEM-1400 electron microscope (Jeol Ltd., Tokyo, Japan) using 100 kV voltage.

## Co-Culturing

NUNC Polycarbonate Cell Culture Inserts with 0.4  $\mu\text{m}$  pore diameter and 3.14  $\text{cm}^2$  culture area (Thermo Fisher Scientific, Waltham, MA, USA) were applied to tumor cell - macrophage co-cultures. 4T1 cancer cells were seeded on the surface of transwell inserts in  $3 \times 10^5$  cells/insert density, while  $6 \times 10^5$ /well J774 cells were seeded into a 6-well plate. In the case of BMDM cells, the cell culture was used on the 7th day, and  $3 \times 10^5$  cells/insert 4T1 cells were seeded on the inserts the day before co-culturing. After 24 hours, 4T1 cells were washed three times with PBS and treated with AuNPs (40  $\mu\text{M}$ ) or AgNPs (20  $\mu\text{M}$ ) in FBS-free HG-DMEM medium. The medium on macrophage cells was also replaced by FBS-free HG-DMEM after washing three times with PBS. The inserts were then transferred into the 6-well plates containing macrophage cells. Tumor cells and macrophages were co-cultured for 24 and 48 hours. The control sample contained macrophages co-cultured with tumor cell-free inserts for 24 and 48 h.

## Reverse Transcription and qPCR

After 24 hours of co-culturing, total cellular RNA was purified from the macrophages by RNeasy® Mini Kit (QIAGEN, Hilden, Germany) according to the manufacturer's recommendation. Two  $\mu\text{g}$  of RNA was reverse transcribed (TaqMan® Reverse Transcription kit, Applied Biosystems, Thermo Fisher Scientific, Waltham, MA, USA) in 50  $\mu\text{L}$  total volume. PCR reactions were performed in PikoReal™ Real-time PCR (Thermo Fisher Scientific, Waltham, MA, USA) using SYBRGreen qPCR Master Mix (Thermo Fisher Scientific, Waltham, MA, USA) with an input of 1  $\mu\text{L}$  cDNA. Relative transcript levels were determined by the  $\Delta\Delta\text{Ct}$  analysis using  $\beta$ -actin as a reference gene. Primer sequences can be found in [Supplementary Material Table S1](#). Primers of target genes were used in 200 nM concentration, while  $\beta$ -actin was used in 100 nM. Experiments were performed using at least three independent biological replicates.

## Detection of Cytokines by Proteome Profiler Array

J774 and BMDMs were co-cultured with untreated, AuNP- (40  $\mu\text{M}$ ), or AgNP-treated (20  $\mu\text{M}$ ) 4T1 cells for 48 h in 6-well plates, and cell culture supernatants were collected from at least 3 independent experiments. The samples were centrifuged for 5 min at  $3,000 \times g$ , and 4 mL of the supernatant was concentrated to approximately 200  $\mu\text{L}$  volume by centrifugation for 30 min at  $7,500 \times g$  using a centrifugal filter (Amicon Ultra-4, UFC800324; Sigma-Aldrich, St. Louis, MO, USA). The Proteome Profiler Mouse Cytokine Array Panel A Kit (R&D Systems, Minneapolis, MN, USA) was applied for multiplex detection of cytokines ([Supplementary Material Table S2](#)). Depicts the coordinates of analytes in the Proteome Profiler (Mouse XL Cytokine) Array). According to the manufacturer's instructions. About 200  $\mu\text{g}$  of protein was used for a single membrane. The chemiluminescent signal was detected by a LICOR C-DiGit (LICOR, Lincoln, NE, USA) Western blot scanner system. The Proteome Profiler Array was assessed with at least three, independent, pooled supernatant samples.

## Migration Assay

Wound healing assays were performed to assess J774 macrophage migration in a direct co-culture. J774 cells were grown in a 2-well silicone insert with a defined cell-free gap (wound healing insert, ibidi GmbH, Grafelfing, Germany) in a 24-well plate. Each insert compartment contained  $7 \times 10^4$  macrophages, and  $2 \times 10^4$  4T1 cells were seeded around the insert in a serum-free medium. After 24 h incubation, while the insert was still in the well, the cells were washed with PBS thrice.

Then, the insert was removed, and the supernatant was replaced by cell culture media without or with nanoparticles (40  $\mu\text{M}$  AuNPs or 20  $\mu\text{M}$  AgNPs). The gap between the J774 cells was imaged by CytoSMART Lux2 (Axion Biosystems, Atlanta, GA, USA) at 0 h (immediately after treatments) and 24 h. The control contained J774 cells seeded into ( $7 \times 10^4$ ) and around the insert ( $2 \times 10^4$ ). HG-DMEM containing 1% FBS was used for the treatments. The device has an algorithm that defines the scratch area and its size in  $\mu\text{m}^2$ . Based on the recorded data, the migration activity was calculated using the formula  $(\text{cell-free area } t_0 - \text{cell-free area treatment time} / \text{cell-free area } t_0 \text{ of control} - \text{cell-free area } t_0 \text{ of control treatment time}) \times 100$ . As a control experiment, the same protocol and data analysis were repeated in case of the untreated and the nanoparticle-treated J774 cells in monoculture.

## Enzyme-Linked Immunosorbent Assay (ELISA)

The in vitro cytokine production of macrophage cells was measured by ELISA. J774 and BMDM cells were co-cultured with 4T1 cells for 24 or 48 hours in 6-well plates, and cell culture supernatants were collected from at least 3 independent experiments. The medium was collected from the macrophages after the co-culture and centrifuged for 5 min at  $3,000 \times g$ , and 4 mL of the supernatant was concentrated to approximately 200  $\mu\text{L}$  by centrifugation for 30 min at  $7,500 \times g$  using a centrifugal filter (Amicon Ultra-4, UFC800324; Sigma-Aldrich, St. Louis, MO, USA). The concentrated samples were adjusted to the same volume. The concentrations of CCL3 and CCL2 in supernatants were determined by commercial ELISA kits (R&D Systems, Minneapolis, MN, USA; catalog nos. DY479, DY450) following the manufacturer's instructions. Absorbance measurement was carried out at 450 nm using the SPECTROstar Nano microplate reader (BMG Labtech, Ortenberg, Germany).

## MMP Activity Assay

According to the manufacturer's instructions, the total matrix metalloproteinase (MMP) activity was measured using the MMP activity assay kit (Abcam, Cambridge, UK; ab112146). After 24 or 48 hours of co-culture, the medium was collected from the macrophages and centrifuged for 5 min at  $3,000 \times g$ , and 4 mL of the supernatant was concentrated to approximately 200  $\mu\text{L}$  by centrifugation for 30 min at  $7,500 \times g$  using a centrifugal filter (Amicon Ultra-4, UFC800324; Sigma-Aldrich, St. Louis, MO, USA). The concentrated samples were adjusted to the same volume. The activities of the MMPs were measured with a fluorescence plate reader at excitation/emission wavelengths of 490/525 nm. Experiments were performed using at least three independent biological replicates.

## Statistical Analysis

Statistical analysis was conducted using GraphPad Prism 8.0 software. All experiments were performed at least three times. When necessary, each replicate was normalized to its own control value, followed by a statistical analysis of the normalized data. Data were expressed as mean  $\pm$  standard deviation (SD). Ordinary one-way ANOVA with Dunnett's or Tukey's multiple comparison test was used with a 95% confidence interval to determine statistical significance (see figure legends for details), and differences between groups were considered significant at  $P$  values of  $<0.05$  (see [Supplementary Material Table S3](#) for the exact  $P$  and confidence interval values, and the number of biological replicates of each experiment).

## Results

### Synthesis and Characterization of AuNPs and AgNPs

AuNPs and AgNPs were prepared using a chemical reduction approach resulting in 128 ppm (1.1866 mM) concentration for AgNPs and 117 ppm (0.594 mM) for AuNPs. The produced nanoparticles were characterized by TEM, dynamic light scattering (DLS), and UV-Vis. Particle morphology and size of the synthesized AuNPs and AgNPs were determined by TEM image analysis ([Figure 1A](#)). According to the obtained TEM micrographs, AuNPs were almost monodispersed, well-separated, and quasi-spherical with a narrow size distribution ( $5.2 \pm 0.6$  nm). AgNPs were also quasi-spherical, well separated from each other, only minor polydispersity could be observed ([Figure 1A](#)). The average size of the AgNPs is proved to be  $10.2 \pm 2.5$  nm. Based on DLS, the average hydrodynamic diameter of AuNPs was between 3 and 10 nm,

while that of AgNPs was between 5 and 20 nm (Figure 1B), which were slightly larger than the core sizes observed in TEM images (5 nm for AuNPs and 10 nm for AgNPs). This difference can be attributed to the solvation layer and possible aggregation in solution, which are detected by DLS but not observed in the dry state of TEM imaging. The zeta potentials of both nanoparticles were highly negative (AuNP:  $-42.9 \pm 5$  and AgNP:  $-43.3 \pm 5$  mV), indicating a negative surface charge that provides stability for the colloid solution. The UV–Vis spectra of the synthesized nanoparticles confirmed their optical properties, with the localized surface plasmon resonance (LSPR) peaks observed at 530 nm for AuNPs and 400 nm for AgNPs, which are consistent with previously reported values for quasi-spherical nanoparticles of similar size (Figure 1C).

## The Cytotoxic Effect of AuNPs and AgNPs on Cancer Cells

To assess the cytotoxicity of the nanoparticles, MTT assays were executed on 4T1 murine breast cancer cells treated with AuNPs or AgNPs (Figure 2A). Dose–response curves were fitted on the obtained viability data (Supplementary material Figure S2), and the corresponding  $IC_{50}$  values were calculated (AuNP  $IC_{50}$   $142.9 \pm 1.08$   $\mu$ M; AgNP  $IC_{50}$   $74.45 \pm 1.07$   $\mu$ M). Based on these measurements, the following concentrations were selected to be applied in further experiments: 40  $\mu$ M for AuNPs and 20  $\mu$ M for AgNPs. These concentrations were low enough to be only slightly toxic to 4T1 cells, which were aimed to be co-cultured with macrophages; nevertheless, they were not toxic at all when applied directly on J774 macrophages (Supplementary material Figure S3). The TEM images taken of AgNP or AuNP-treated cancer cells demonstrated that the nanoparticles were taken up and accumulated in the cytoplasm of 4T1 cells (Figure 2B). J774 macrophages are also taking up the nanoparticles when they are exposed to them directly (Supplementary material Figure S3).

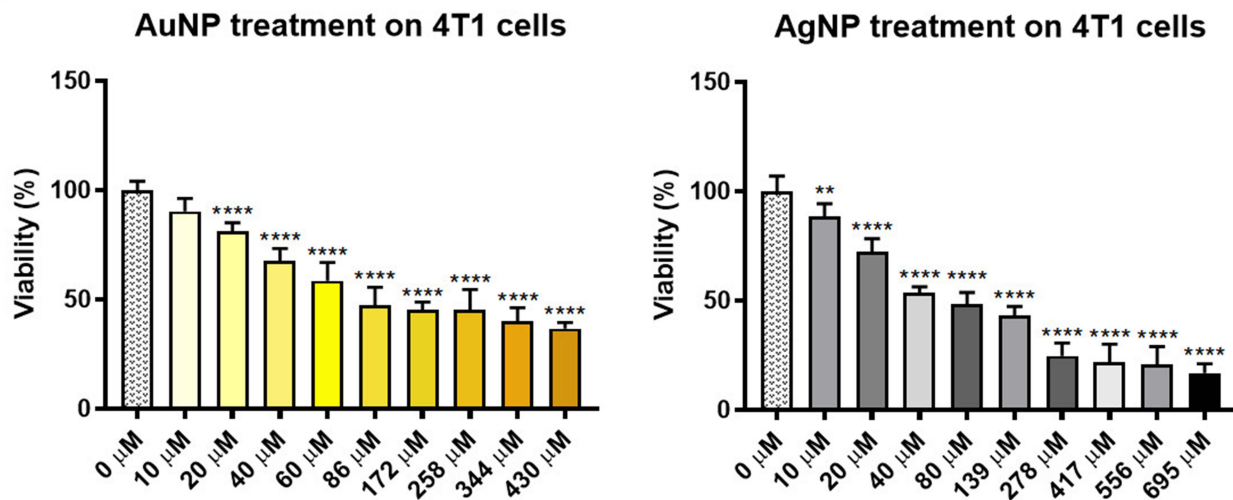
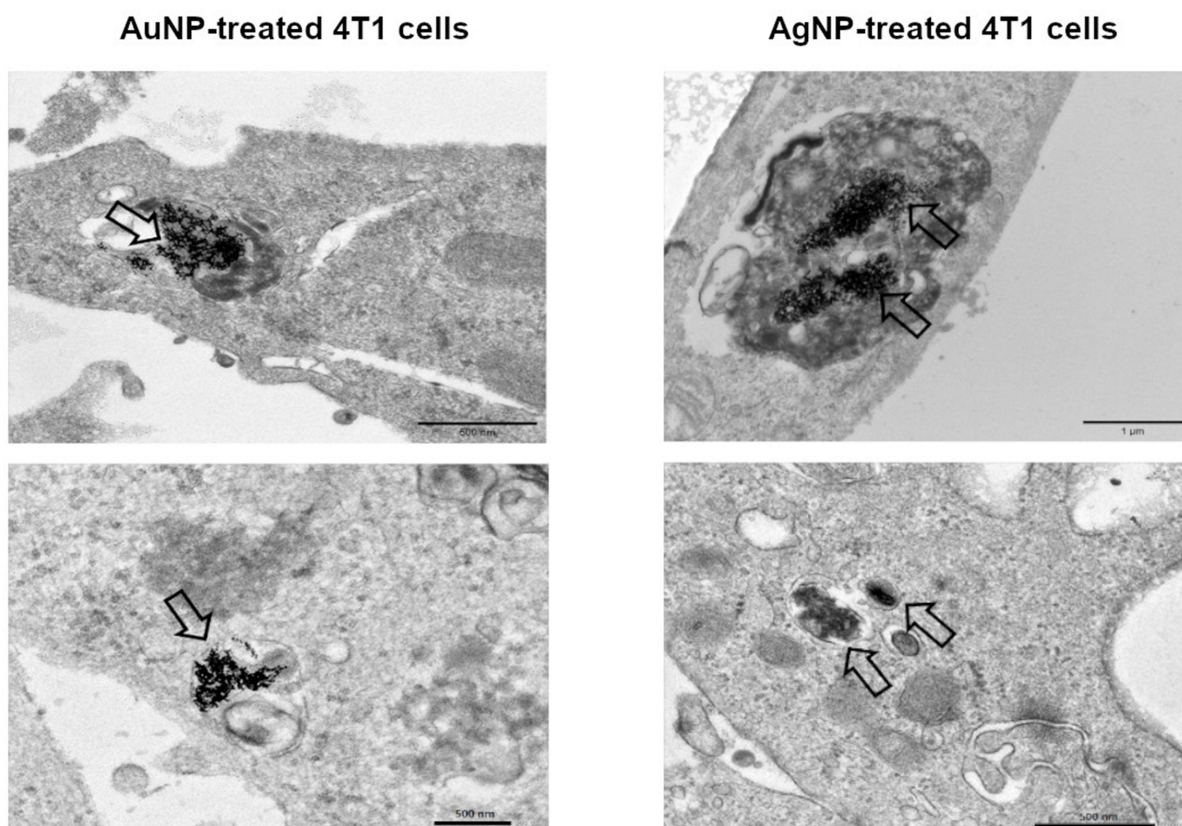
## AuNPs and AgNPs Indirectly Modulate the Relative Expression of Macrophage Polarization and Functional Marker Genes

To investigate the indirect effect of AuNPs and AgNPs on macrophage-tumor cell paracrine communication, we established insert-based co-cultures of 4T1 breast cancer and J774 macrophage cell lines, where the two cell types co-exist but are also separated, and their secreted, soluble molecules are able to pass the insert pores and thereby influence one another. Since we aimed to examine the indirect modulatory effect of AuNPs and AgNPs, cancer cells were treated with either of the nanoparticles in parallel wells. For most experiments, four types of samples were created: 1. monoculture of macrophages (control), 2. co-culture of macrophages with untreated tumor cells (co-culture with 4T1s), 3. co-culture of macrophages with AuNP-treated tumor cells (co-culture with AuNP-treated 4T1s) and 4. co-culture of macrophages with AgNP-treated tumor cells (co-culture with AgNP-treated 4T1s). After 24 h co-culturing, total RNA was isolated from macrophage cells and reverse transcribed, and then qPCR was performed.

First, we examined the mRNA expression levels of various M1-like and M2-like TAM phenotype marker genes in J774 cells. In J774 cells that were co-cultured with 4T1s for 24 h, a significantly increased mRNA level of most investigated markers (*Il-23*, *Ccl22*, *Ccl2*, *Cd206*, *Tgf- $\beta$* , *Cox2*, *Nos2*, *Mmp9*) was observed compared to the monoculture macrophage control (Figure 3), verifying an active communication between cancer and macrophage cells and supporting a cancer cell-induced macrophage reprogramming in our co-culture system. When 4T1 cells were treated with AuNPs or AgNPs, and these cancer cells were co-cultured with the macrophages, significantly lower expression levels of many of the above-mentioned markers (*Il-23*, *Ccl22*, *Ccl2*, *Cd206*, *Tgf- $\beta$* , *Nos2*, *Mmp9*) were measured compared to the untreated co-culture samples, indicating a possible indirect modulatory effect of metal nanoparticles on macrophages. Comparing the impact of the two nanoparticles, for certain marker genes, AuNPs (*Il-23*, *Ccl22*) and in other cases (*Cd206*, *Nos2*, *Cox2*, *Mmp9*), AgNPs seemed to be more efficient. Interestingly, the expression of *TNF- $\alpha$*  increased significantly in the presence of AuNPs and AgNPs (Figure 3).

Besides the immortalized J774 macrophage cell line, we included primary macrophage cells derived from mouse bone marrow (BMDM) in our study and examined whether they behave in the same way under similar conditions as J774 cells. BMDM-4T1 co-cultures were established and treated with AuNPs and AgNPs identically as it was in the J774-containing model system. In BMDMs that were exposed to 4T1 cells, a drastic increase in mRNA expression of most



**A****B**

**Figure 2** Cytotoxic effects and internalization of gold (AuNPs) and silver (AgNPs) nanoparticles by 4T1 breast cancer cells. **(A)** The cytotoxicity of metal nanoparticles on 4T1 cells was assessed using a viability assay, and **(B)** internalization of AuNPs and AgNPs in 4T1 cancer cells was verified by transmission electron microscopic analysis (AuNP: left panels, AgNP: right panels). (\*\*P=0.0099, \*\*\*\*P<0.0001, One-way ANOVA; Dunnett's multiple comparisons test, values represent mean  $\pm$  standard deviation (SD)).

markers (*Il-23*, *Ccl22*, *Ccl2*, *Cd206*, *Tgf- $\beta$* , *Cox2*, *Nos2*, *Mmp2*, *Mmp9*) was observed compared to those of the control BMDM (Figure 4). When 4T1 cells of the co-culture were exposed to AuNPs or AgNPs, the expression levels of many examined genes (*Chil3*, *Il-23*, *Ccl22*, *Ccl2*, *Cd206*, *Tgf- $\beta$* , *Cox2*, *Nos2*, *Mmp2*, *Mmp9*) were significantly lower compared to the expressions obtained from the untreated co-culture. These data further strengthen the potential of metal



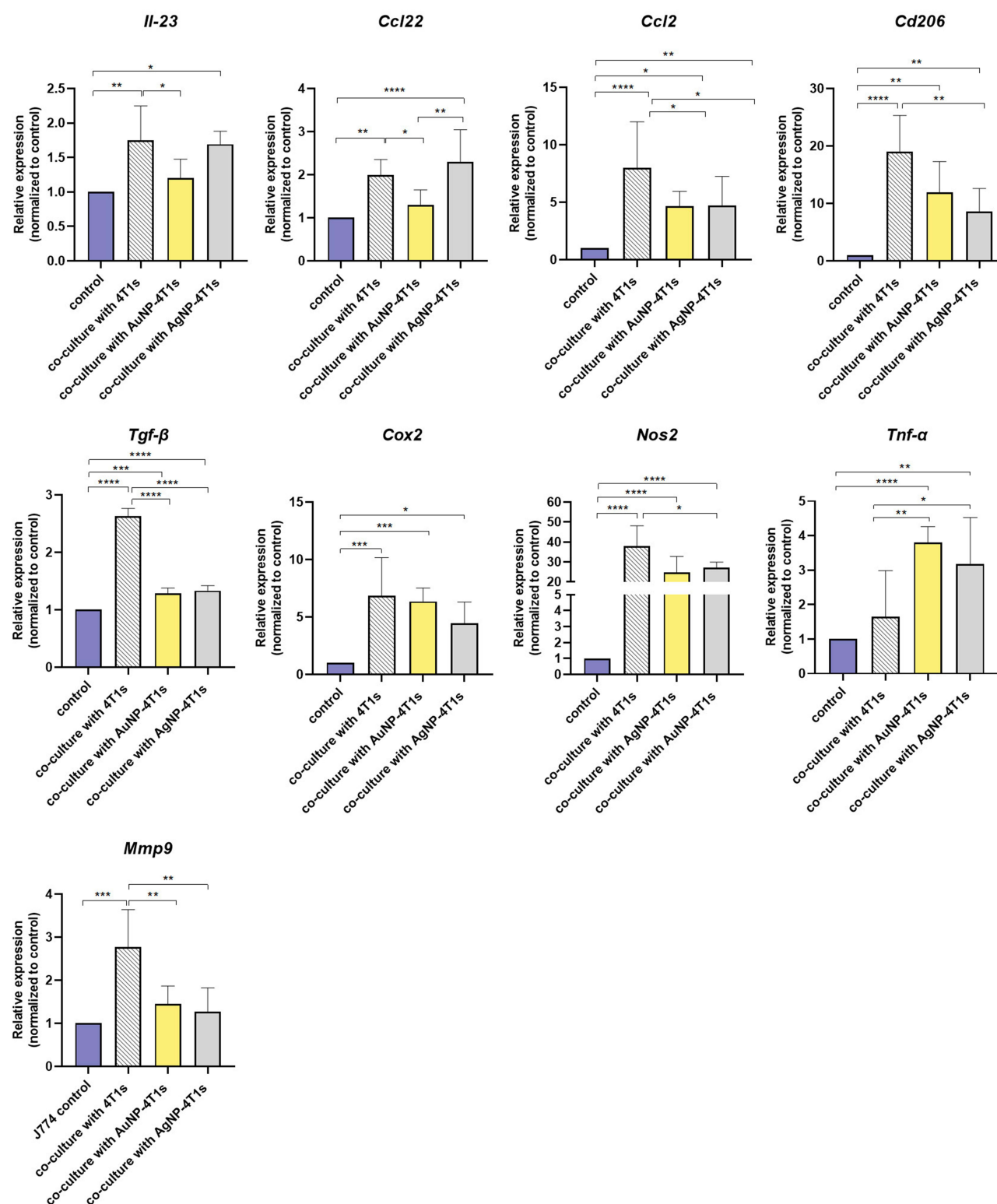


**Figure 3** Relative expression levels of various polarization and functional marker genes in J774 macrophages. Gene expression was examined in monocultured J774 cells (J774 control), as well as in J774 cells co-cultured with untreated, or gold (AuNP)-, or silver (AgNP) nanoparticle-treated 4T1 breast cancer cells, determined by RT-qPCR (control: monoculture of J774 cells, co-culture with 4T1s: J774 cells co-cultured with untreated 4T1 cells, co-culture with AuNP-treated 4T1s: J774 cells co-cultured with AuNP-treated 4T1 cells, co-culture with AgNP-4T1s: J774 cells co-cultured with AgNP-treated 4T1 cells).

**Notes:** \* $P \leq 0.0383$ , \*\* $P \leq 0.0086$ , \*\*\* $P \leq 0.0006$ , \*\*\*\* $P < 0.0001$ , One-way ANOVA; Tukey's multiple comparisons test, values represent mean  $\pm$  standard deviation (SD).

**Abbreviations:** *Il-23*, interleukin-23; *Ccl22*, C-C motif chemokine ligand 22; *Ccl2*, C-C motif chemokine ligand 2; *Cd206*, macrophage mannose receptor; *Tgf-β*, transforming growth factor-beta; *Cox2*, cyclooxygenase-2; *Nos2*, inducible nitric oxide synthase; *Tnf-α*, tumor necrosis factor-alpha; *Mmp9*, matrix metalloproteinase 9.

nanoparticles to attenuate the tumor-supporting reprogramming action of cancer cells forced on stromal cells. Interestingly, AuNPs performed better in suppressing the expression of *Chil3*, *Mmp2*, and *Mmp9*, whereas AgNPs proved to be more potent in this respect for *Ccl2* gene expression (Figure 4). It is noteworthy that the expression levels of several MMP genes were reduced upon the nanoparticle treatments during the co-culture of both J774 as well as BMDM-containing systems, implying that modulation of the migration capacity and extracellular matrix (ECM) remodeling capability of TAM-like cells is a rational presumption in nanoparticle-based approaches. Based on the observed gene expression profiles of both primary and immortalized macrophages, we can clearly state that the presence of tumor cells enhances the expression of TAM-like markers in macrophages, and importantly, nanoparticle treatments are capable of suppressing these cancer-induced expressional changes, suggesting a strong impact of metal nanoparticles in the attenuation of the stroma cell modulatory program in cancer cells.

## The Secretion of Certain Soluble Factors by Macrophages Is Affected by the Presence of Cancer Cells and by Nanoparticle Treatments

Macrophages are generally characterized by robust cytokine expression and secretion. As we have seen that cancer cells and metal nanoparticles can influence the gene expression profile of immortalized J774 and primary BMDM macrophages, therefore, we aimed to examine what happens with their cytokine secretion under the influence of 4T1 cells and AuNP- or AgNP-treated cancer cells. For this purpose, the cytokine, chemokine, and other soluble factor profiles of J774 and BMDM cells were examined by the Proteome Profiler Array. Although several of the above-mentioned factors were found to be secreted and present in the supernatants of both J774 and BMDM cells, the BMDM supernatants had a significantly higher number of detected targets than the J774 samples (Supplementary material Figure S4 and Figure S5). Upon exposure of the macrophages to 4T1 cancer cells and metal nanoparticle-treated 4T1 cells, the protein levels of many soluble factors were altered in both BMDM and J774 supernatants based on the Proteome Profiler Arrays. Importantly, the observed alterations in the protein levels corresponded to the changes in the mRNA expressions measured by RT-qPCR.

More specifically, the protein levels of some targets (IL-23, CCL22, TNF- $\alpha$ , MMP9) in the J774 supernatants of macrophages that were co-cultured with AgNP-treated 4T1 cells were lower than those in the untreated co-cultured macrophage supernatants. In AuNP-exposed co-cultures, CCL22 protein expression of J774 cells resulted to be lower; however, the CCL2 protein level was elevated in J774 supernatants compared to those macrophages that were in the untreated co-culture sample. Interestingly, the Proteome Profiler Array did not detect any MMP9, TNF- $\alpha$ , or IL-23 signal in J774 monocultures and also no IL-23 in the AgNP-exposed co-cultures (Figure 5).

In supernatants of BMDMs co-cultured with 4T1 cells, protein levels of IL-23, *Chil3*, CCL2, MMP2, and MMP9 were higher compared to control BMDM supernatants. As expected, AuNPs and AgNPs affected the secreted protein levels, since the expression of certain target proteins (IL-23, *Chil3*, CCL2, MMP2, MMP9) was lower in BMDMs that were cultured together with nanoparticle-treated cancer cells than in untreated co-culture samples (Figure 6). However, in the case of *Chil3*, the effect of AuNP exposure was more potent than that of AgNPs in the co-culture samples.

The protein profiles of both J774 and BMDM supernatants suggest that although 4T1 cells can induce an elevation in the protein expression of TAM-like markers in macrophages, nanoparticle treatments are able to influence this modulatory effect of cancer cells, leading to an attenuated expression and/or secretion of certain cytokines, chemokines, soluble factors, eg TAM-like markers. These results correspond to those we obtained by RT-qPCR.

## The Presence of Cancer Cells and the Nanoparticle Treatments Both Influence the Migration of Macrophages

The RT-qPCR and Proteome Profiler Array analyses demonstrated that mRNA expression and the amount of secreted proteins of some chemokines (CCL2, CCL3) and MMPs (MMP2 and MMP9) were changed upon co-culturing macrophages with cancer cells and again modified by nanoparticle treatments. Since these factors are crucial for cell migration and motility, further experiments were performed to investigate the migratory capacity, the activity of secreted MMPs, and the quantity of certain migration-related chemokines in J774 macrophages. During the migration assay,

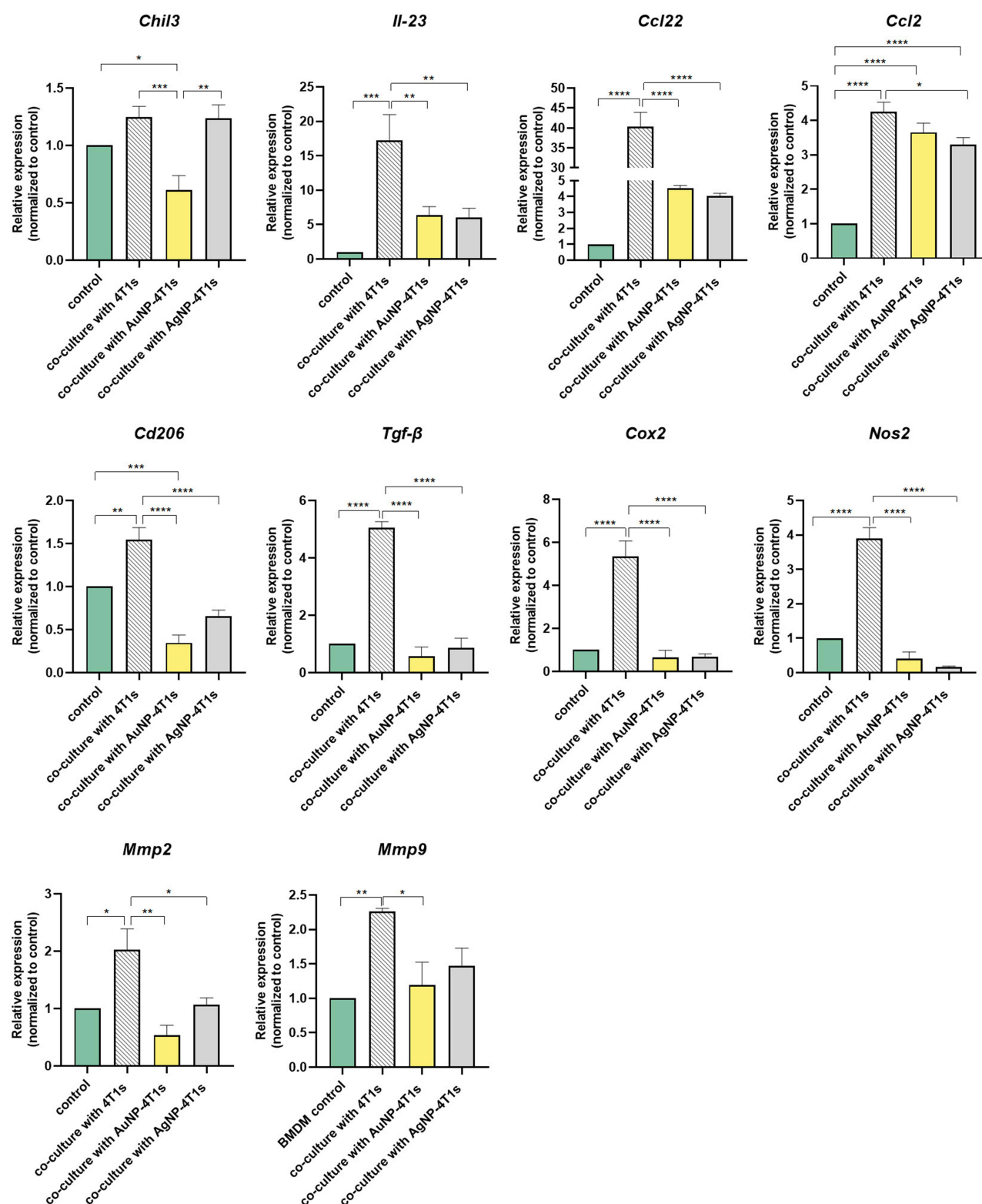


**Figure 4** Relative expression levels of various polarization and functional marker genes in primary bone-marrow-derived macrophage (BMDM) cells maintained in monoculture (control) or in co-culture with untreated, gold (AuNP)-, or silver (AgNP) nanoparticle-treated 4T1 breast cancer cells determined by RT-qPCR (control: monoculture of BMDM cells, co-culture with 4T1s; BMDM cells co-cultured with untreated 4T1 cells, co-culture with AuNP-treated 4T1s; BMDM cells co-cultured with AuNP-treated 4T1 cells, co-culture with AgNP-4T1s; BMDM cells co-cultured with AgNP-treated 4T1 cells).

**Notes:** \* $P \leq 0.0492$ , \*\* $P \leq 0.0074$ , \*\*\* $P \leq 0.0009$ , \*\*\*\* $P < 0.0001$ , One-way ANOVA; Tukey's multiple comparisons test, values represent mean  $\pm$  standard deviation (SD).

**Abbreviations:** *Chil3*, chitinase-like-3 protein; *Il-23*, interleukin-23; *Ccl22*, C-C motif chemokine ligand 2; *Ccl2*, C-C motif chemokine ligand 2; *Cd206*, macrophage mannose receptor; *Tgf-β*, transforming growth factor-beta; *Cox2*, cyclooxygenase-2; *Nos2*, inducible nitric oxide synthase; *Mmp2*, matrix metalloproteinase 2; *Mmp9*, matrix metalloproteinase 9.

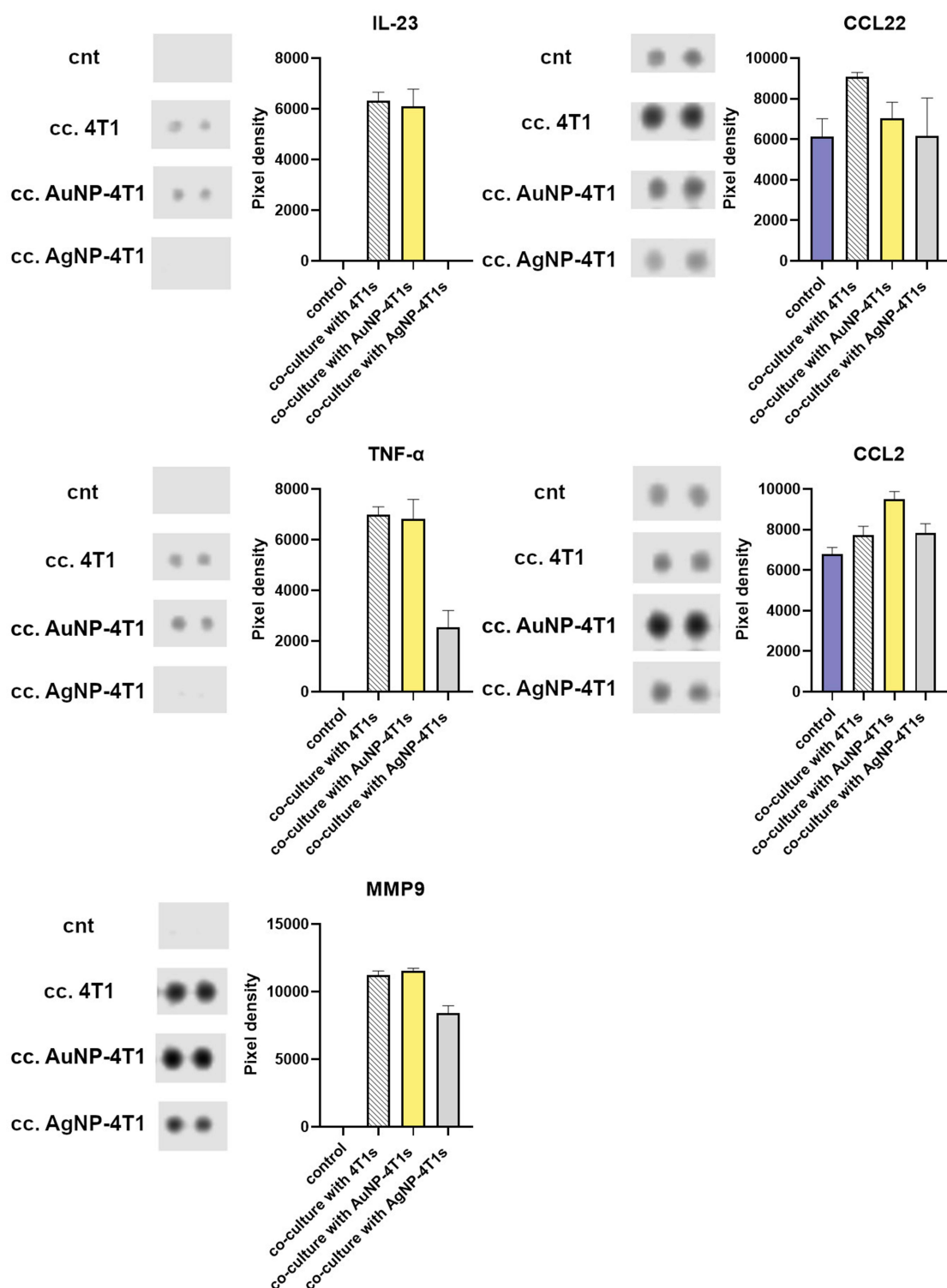


**Figure 5** Relative amounts of selected cytokines, chemokines, and soluble factors secreted by J774 macrophages upon exposure to cancer cells and metal nanoparticles. The relative quantity of these proteins was assessed in J774 supernatants collected from macrophage monocultures or from co-cultures with 4T1 breast cancer cells by Proteome Profiler Array. Representative pictures and quantification of target dots based on chemiluminescence intensity are presented. Values represent mean  $\pm$  standard deviation (SD) calculated from the intensity of two dots/target. (cnt: monoculture of J774s control, cc. 4T1: J774s co-cultured for 48 hours with untreated 4T1 cells, cc. AuNP-4T1: J774s co-cultured for 48 hours with AuNP-treated 4T1 cells, cc. AgNP-4T1: J774s co-cultured for 48 hours with AgNP-treated 4T1 cells).

**Abbreviations:** IL-23, interleukin-23; CCL22, C-C motif chemokine ligand 22; TNF- $\alpha$ , tumor necrosis factor- $\alpha$ ; CCL2, C-C motif chemokine ligand 2; MMP9, matrix metalloproteinase 9.

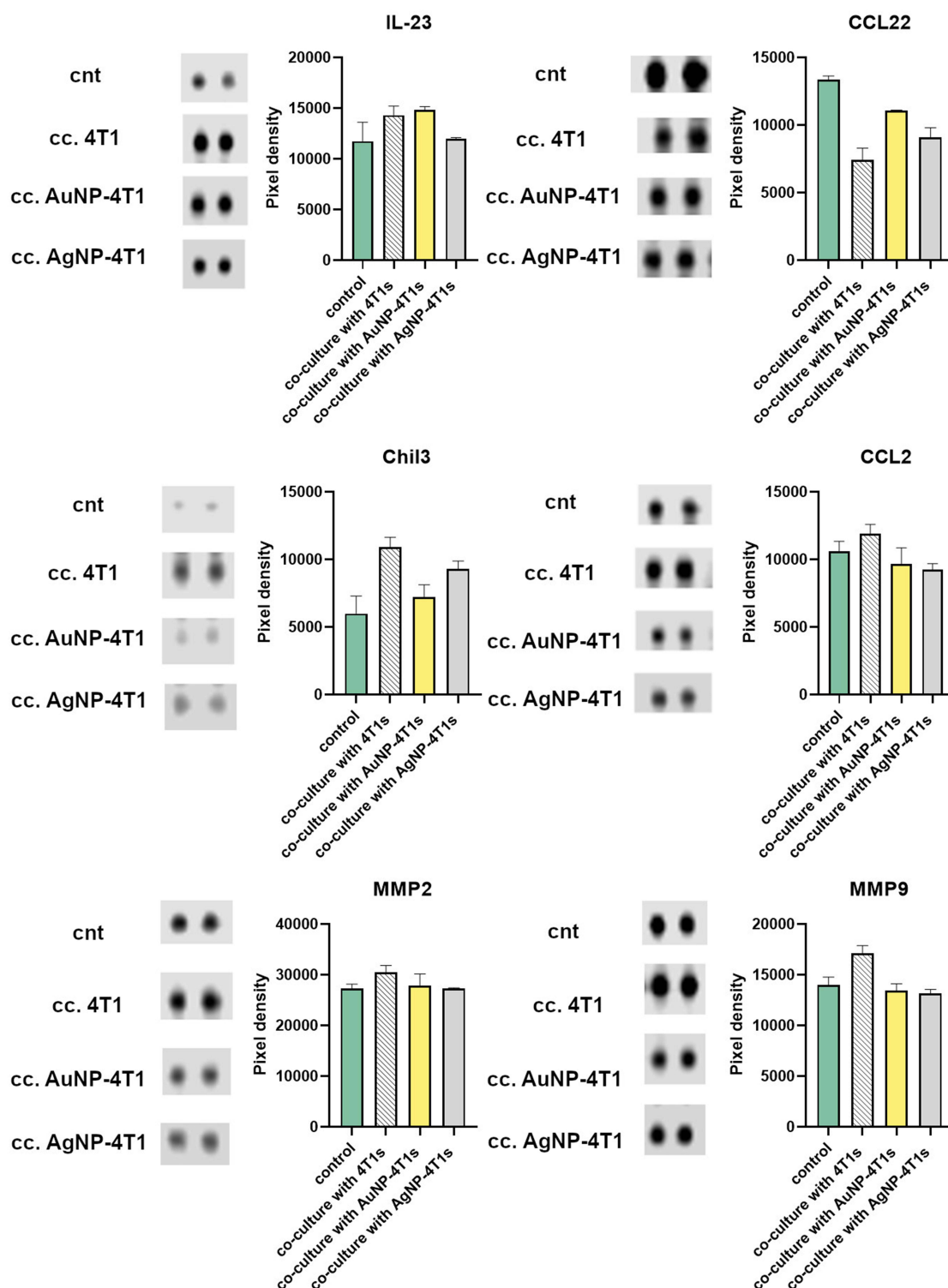


**Figure 6** Relative amounts of selected cytokines, chemokines, and soluble factors secreted by primary bone-marrow-derived macrophages upon exposure to cancer cells and metal nanoparticles. The relative quantity of these proteins was assessed in primary bone-marrow-derived macrophage (BMDM) supernatants collected from macrophage monocultures or from co-cultures with 4T1 breast cancer cells by Proteome Profiler Array. Representative pictures and quantification of target dots based on chemiluminescence intensity are presented. Values represent mean  $\pm$  standard deviation (SD) calculated from the intensity of two dots/target. (cnt: monoculture of BMDMs control, cc. 4T1: BMDMs co-cultured for 48 hours with untreated 4T1 cells, cc. AuNP-4T1: BMDMs co-cultured for 48 hours with AuNP-treated 4T1 cells, cc. AgNP-4T1: BMDMs co-cultured for 48 hours with AgNP-treated 4T1 cells).

**Notes:** **Abbreviations:** IL-23, interleukin-23; CCL22, C-C motif chemokine ligand 22; Chil3, chitinase-like-3 protein; CCL2, C-C motif chemokine ligand 2; MMP2, matrix metalloproteinase 2; MMP9, matrix metalloproteinase 9.



macrophages and cancer cells were placed in a direct co-culture, and macrophage migration was tested using a wound healing insert. In parallel experiments, the co-cultures were treated with nanoparticles. Based on the 24 h migration assay, the migratory capacity of J774 cells in the presence of cancer cells was significantly higher than those of J774 in monoculture. Upon AuNP or AgNP treatments, the movement of J774 cells was decreased significantly compared to the untreated co-culture (Figure 7A and B). As a control experiment, we examined whether a direct AuNPs or AgNPs treatment of J774 cells in a monoculture setup would influence the macrophage migratory capacity. We found that the nanoparticles did not affect J774 migration significantly (Supplementary Material Figure S6). CCL2 and CCL3 have an important role in cell recruitment and infiltration. Upon examination of their quantities by ELISA, we found that the amount of these molecules was elevated in the supernatants of the 4T1-J774 co-culture samples compared to the J774 monoculture (control). As expected, the nanoparticle treatments induced a significant reduction in the concentration of these factors; their level was similar to that of the control (Figure 7C). In the case of CCL2, both AuNPs and AgNPs diminished significantly the amount of the soluble proteins; however, in the case of CCL3, only AgNP treatment

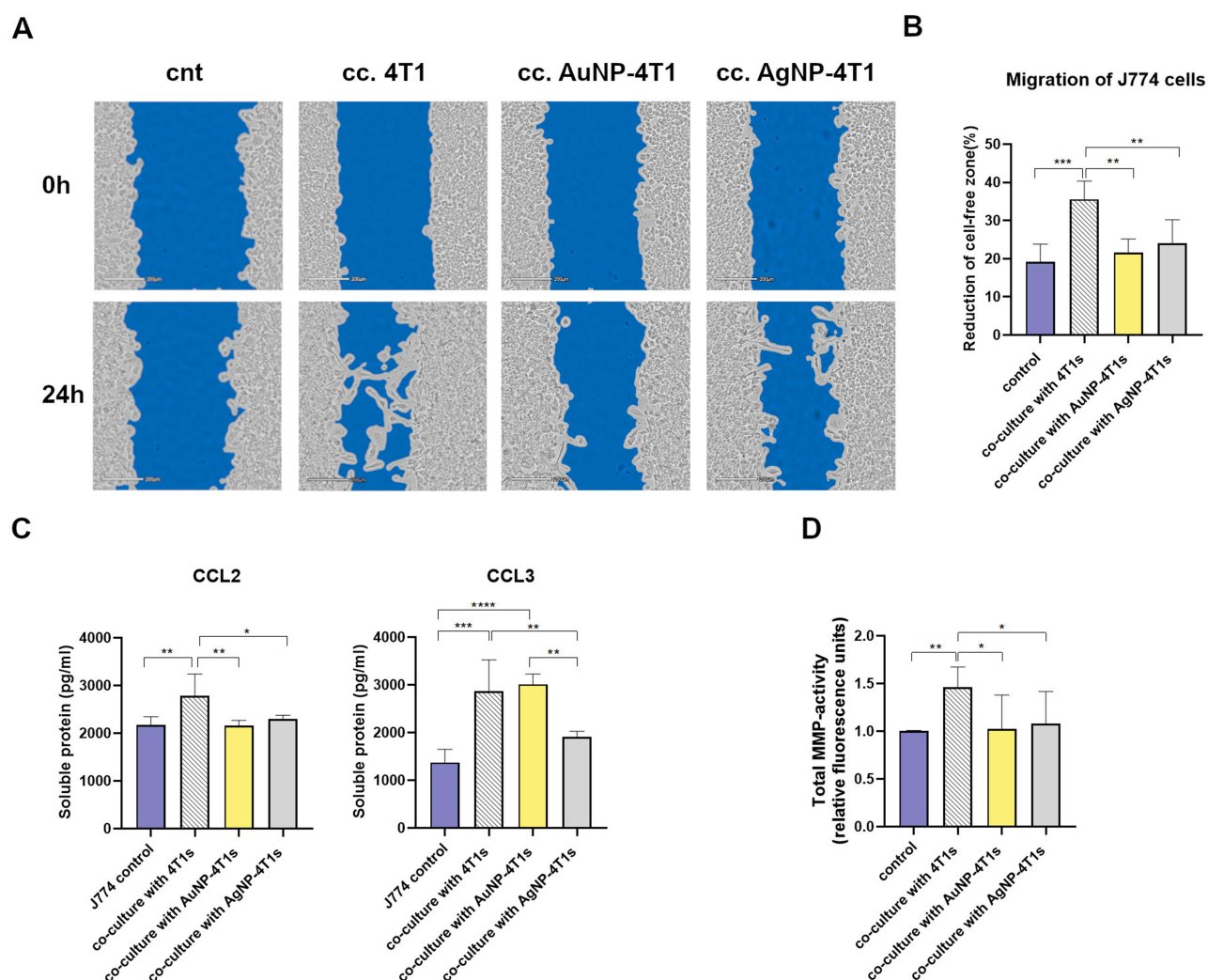


**Figure 7** The presence of cancer cells and also nanoparticles affects the migratory capacity of J774 macrophages. **(A)** Representative images and **(B)** the quantified migratory capacity of J774 cells after 24 h co-culturing with 4T1 breast cancer cells and nanoparticle treatments. **(C)** Quantity of chemokines C-C motif chemokine ligand 2 (CCL2) and C-C motif chemokine ligand 3 (CCL3) measured by Enzyme-Linked Immunosorbent Assay (ELISA) from supernatants of J774 cells co-cultured for 24 hours with untreated or metal nanoparticle-treated 4T1 cancer cells. **(D)** The activity of J774-secreted matrix metalloproteinase (MMP) enzymes was detected by Total MMP activity assay from 24 h co-culture supernatants (control: monoculture of J774 cells, co-culture with 4T1s; J774 cells co-cultured for 24 hours with untreated 4T1 cells, co-culture with AuNP-treated 4T1 cells, co-culture with AgNP-4T1s; J774 cells co-cultured for 24 hours with AgNP-treated 4T1 cells). (\* $P < 0.0370$ , \*\* $P < 0.0097$ , \*\*\* $P < 0.0004$ , \*\*\*\* $P < 0.0001$ , One-way ANOVA; Tukey's multiple comparisons test, values represent mean  $\pm$  standard deviation (SD)).

appeared efficient (Figure 7C). The total MMP activity in the supernatants of mono- and with cancer cells co-cultured J774 cells was also investigated since these enzymes are directly responsible for the modulation of macrophage motility and ECM remodeling. The total MMP enzyme activity was significantly elevated in the 4T1-J774 co-culture sample compared to the J774 monoculture; however, both AuNP and AgNP treatments reduced the total MMP activity of J774 cells in 4T1 co-cultures (Figure 7D). These results all imply that the presence of cancer cells positively modulates the macrophage migration capacity and matrix remodeling activity, probably as a part of the cancer-induced reprogramming regimen on stromal macrophages. Importantly, when cancer cells are exposed to metal nanoparticles, the mobility and matrix metalloprotease activity of the macrophages in the vicinity of these cancer cells become significantly suppressed, further supporting the counterbalancing role of metal nanoparticles in this particular milieu.

## Discussion

In this study, we explored the impacts of AuNPs and AgNPs on the paracrine communication between murine macrophages (J774 or BMDM) and breast cancer cells (4T1) in an insert-based in vitro co-culture system, focusing on how these metal nanoparticles influence macrophage reprogramming by cancer cells.

Macrophages are essential components of the TME with high adaptation capacity, depending on the type of modulatory signals they encounter. These cells might shift their polarization, lose their antitumor effector functions, and become facilitators of tumor progression and invasion. There are key molecules such as chemokines, cytokines, and various enzymes, expressed and secreted by macrophages that are denoting a modulation of phenotype, polarization, and behavior in these cells. Therefore, in this study, we tried to identify and track the changes in the expression of such marker molecules in macrophage cells upon exposing them to metal nanoparticle-treated cancer cells.

Among chemokines, CCL22 is understood to be rather relevant regarding macrophages. CCL22, produced primarily by macrophages and dendritic cells (DCs), serves as a chemoattractant for CD4 and CD8 T-cells, IL-2-activated natural killer (NK) cells, has also relevance in chronic inflammation and promoting regulator T cell (Treg) infiltration into the TME, thereby contributing to tumor immunosuppression and reduced antitumor immunity.<sup>57,58</sup> It was previously shown that TAMs produce an excessive amount of CCL22, and the level of this chemokine in the tumor stroma was positively associated with the amount of intratumoral phospho-focal adhesion kinase (pFAK Tyr397), which in turn correlated with increased tumor metastasis, and with reduced patient survival.<sup>59</sup> Another significant chemokine that seems to be a key factor in influencing macrophage polarization towards M1 or M2 types context-dependently is CCL2.<sup>60</sup> Although it has been linked to antitumor effects via myeloid cell activation,<sup>61</sup> it is also associated with tumor progression through M2 polarization, immunosuppression, enhanced tumor survival, and metastasis; moreover, elevated CCL2 levels also correlated with poor prognosis in breast and lung cancer.<sup>60</sup> Based on these reports, we examined the expression levels of these two chemokines, and although elevated *Ccl2* and *Ccl22* mRNA levels were found in both J774 and BMDM macrophages that were co-cultured with untreated 4T1 cells, AuNP or AgNP treatments led to diminished expression of *Ccl2* and *Ccl22* in both macrophage-containing co-culture samples. These results were supported by the respective changes in protein levels determined by the Proteome Profiler Array on BMDM and J774 co-culture samples. These findings suggest that metal nanoparticles can indirectly attenuate the level of key chemokines, such as CCL2, thereby helping to inhibit tumor growth, while the suppression of CCL22 could influence immune cell infiltration into the TME.

Naturally, apart from chemokines, the expression and secretion of crucial cytokines were also examined in macrophages of the co-culture system. For example, IL-23, a member of the IL-12 superfamily of cytokines, was previously shown to promote tumor growth and metastasis controlled by M2 macrophages, affecting neutrophil-mediated immunity,<sup>62</sup> secretion of immunosuppressive cytokines such as TGF- $\beta$ , IL-10, and vascular endothelial growth factor into tumor tissues, and inducing the secretion of MMP9,<sup>62</sup> via downstream signaling of the Janus kinase–signal transducers and activators of the transcription (JAK-STAT) pathway, involving both STAT3 and STAT4.<sup>63</sup> In our study, we found higher gene and protein expression of IL-23 in both J774 and BMDMs co-cultured with cancer cells, which was reduced significantly by AuNP and AgNP treatments. Adhering to the observations made above on chemokines, it seems that the tumor-promoting functions of IL-23 can also be substantially reduced by metal nanoparticles, and thereby, the reprogramming activity of cancer cells exerted on macrophages can be perturbed.

Another critical and rather versatile cytokine produced by macrophages is TNF- $\alpha$ .<sup>64</sup> Considered as a double-edged sword in cancer, TNF- $\alpha$  could exert antitumor effects by inducing apoptosis, promoting M1 polarization of TAMs, attracting immune cells to tumor sites, and disrupting tumor vasculature.<sup>65,66</sup> Conversely, it can act as a pro-tumoral cytokine, supporting cell proliferation, tumor progression, epithelial-to-mesenchymal transition, angiogenesis, and metastasis in various cancers.<sup>67</sup> Studies indicated that the behavior of TNF- $\alpha$  depends mostly on the specific cellular context.<sup>68,69</sup> In the case of some estrogen receptor-positive breast cancer cell lines, TNF- $\alpha$  promoted both proliferation and survival. In T47D cells, stimulation of the TNF receptor 1 induced weak Jun N-terminal kinase (JNK) signaling and strong activation of the PI3-K/AKT pathway, which in turn led to the stimulation of the NF- $\kappa$ B complex, enhanced the expression of cyclin D1 and BCL-XL, and promoted tumor growth.<sup>70,71</sup> On the other hand, TNF- $\alpha$  was shown to promote apoptosis in certain breast cancer types.<sup>72–74</sup> In MCF-7 adenocarcinoma cells, the TNF- $\alpha$ -induced apoptosis occurred in a poly-ADP-ribose polymerase- and caspase-dependent way,<sup>75</sup> by induction of the DISC-complex formation (apoptosis signaling by extrinsic pathway) and by promoting cytochrome c release from the mitochondria (apoptosis signaling by intrinsic pathway).<sup>76</sup> In the triple-negative breast carcinoma BT549 cells TNF- $\alpha$  has been found to induce apoptosis through the activation of c-Jun, leading to the down-regulation of 23 anti-apoptotic genes, while 13 pro-apoptotic genes were found to be upregulated.<sup>72</sup> It is important to mention that, apart from the direct activation of apoptotic pathways, TNF- $\alpha$  can exert its antitumor activity through inflammatory and immune responses, and extensive destruction of tumor vasculature,<sup>77</sup> events that are attributed to the activation of antitumor immune cells in the bloodstream, including macrophages, cytotoxic lymphocytes, and neutrophils.<sup>78–81</sup> Acknowledging these contradictory findings, we were not surprised to see that the *Tnf- $\alpha$*  gene expression was significantly elevated in the presence of 4T1 cancer cells, and its expression was even higher upon nanoparticle treatments. Considering the pro-apoptotic and antitumor functions of this cytokine detailed above, it is possible that the increased expression of this cytokine might assist the cancer-eliminating activity of metal nanoparticles in this particular model system; nevertheless, further experiments are required to explore this issue.

NOS2 and COX2 are two enzymes often regarded as key molecular markers to characterize macrophage/TAM phenotype and polarization. TAMs can express NOS2 and generate the gaseous messenger nitric oxide (NO).<sup>82</sup> Utilizing different tumor models both in vitro and in vivo, researchers suggested that NO generated by NOS2 of M2-polarized TAMs can protect tumor cells from apoptosis induced by therapeutic agents, implying that upon chemotherapy, suppression of NO synthesis might be beneficial.<sup>83</sup> Moreover, in macrophages, NO increased the activity of MMP9 via cGMP-dependent suppression of the metalloproteinase inhibitor TIMP1.<sup>84,85</sup> COX2, an inducible enzyme participating in prostanoid synthesis, has also been linked to inflammatory diseases, and cancer, it was suggested to advance angiogenesis, tissue invasion, immune evasion, and resistance to apoptosis and chemotherapy. COX2 can suppress DC and T cells (type 1 immunity) via the PGE2-EPs signaling pathway, and also of cytolytic T cell and NK cell activities through cAMP-dependent mechanisms, however, promotes type-2 immunity, thereby contributing to tumor immune evasion.<sup>86,87</sup> In fact, inhibition of COX was shown to foster pro-inflammatory/antitumor Th1 phenotypes of CD4+ and CD8+ T cells, led to reduced tumor growth and metastatic burden, improved the survival of tumor-bearing mice, and helped to counteract tumor immune evasion.<sup>86,88</sup> In our experiments, we detected elevated *Nos2* and *Cox2* gene expression in J774 and BMDM macrophages co-cultured with untreated 4T1 cells; however, upon AuNP and AgNP treatments, the expression levels of these markers were drastically lowered. According to these findings, suppression of NOS2 and COX2 by metal nanoparticles could reverse the cancer-promoting actions of TAMs, most likely by counteracting the cancer cell proliferation- and survival-supporting, COX2-positive TAMs, described by Li et al.<sup>20</sup> Attenuation of NOS2 and COX2 by nanoparticle treatment might also help to avoid drug resistance by enhancing the apoptotic efficiency of other chemotherapeutic agents.<sup>20</sup> These actions of AgNPs and AuNPs would be highly advantageous in view of a specific crosstalk previously verified between NOS2 and COX2, where the elevated co-expression of these factors was associated with an aggressive breast cancer phenotype, and predicted significantly reduced patient survival.<sup>89</sup> According to these reports, an increased NO level induces COX2, and the elevated level of PGE2 induces NOS2, which ultimately stimulates several oncogenic pathways such as ERK, PI3K, NF- $\kappa$ B, and AP1. Concomitantly, PGE2 increased IL-10 and TGF- $\beta$  Th2 cytokines, which blocked DC maturation and antigen presentation.<sup>87</sup> This feedforward signaling of NOS2/COX2 resulted in a chronically immunosuppressed tumor immune microenvironment.<sup>89</sup>

We hypothesized that metal nanoparticle treatment can perturb the M2-like polarization forced on TAMs by cancer cells. Therefore, we tracked the variations in M2 marker expression between the experimental groups. M2-like TAMs generally express a high level of CD206, a C-type lectin macrophage mannose receptor, that has been implicated in tumor progression and associated with poor disease prognosis.<sup>90,91</sup> In fact, CD206+ TAMs, via the production of epidermal growth factor or upon interactions with CD4+ T cells through MHC-II axis, assisted tumorigenesis and the formation of an immunosuppressive microenvironment.<sup>92,93</sup> Mao et al discovered that elevated levels of CD206 enhanced M2-type polarization of TAMs and stimulated the production of TGF- $\beta$  and IL-6 in tumor tissues, facilitating thereby the progression of hepatocellular carcinoma.<sup>94</sup> Chil3 (or Ym1) is a rodent-specific, non-catalytic chitinase-like protein primarily produced by macrophages and neutrophils. Though its function is not fully understood, Chil3 is widely recognized as a key marker of alternatively activated macrophages in mice and is commonly used to distinguish macrophage phenotypes.<sup>95</sup> It was shown that alternatively activated macrophages, which express Chil3, can stimulate the growth of early pancreatic lesions via secretion of CCL2, IL-1ra and are the primary producers of TGF- $\beta$  in this tumor type.<sup>96–98</sup> TGF- $\beta$  is a ubiquitous modulator of cellular responses, regulating, among others, monocyte activation, cytokine production, host defense, and chemotaxis. TGF- $\beta$  signaling can inhibit cell growth in healthy cells, but it can induce tumor development, including cell proliferation, invasion, immune suppression, and microenvironment modification, a phenomenon known as the TGF- $\beta$  paradox.<sup>99</sup> It is important to point out that many of the pathways discussed in this work, also those involving IL-23, NOS2, and COX2, culminate into increased expression of TGF- $\beta$ . As a consequence, in the late malignant stage of cancers, TGF- $\beta$  ultimately acts as a tumor promoter by activating the TGF- $\beta$  receptor/SMAD pathway. Studies have revealed that TGF- $\beta$  plays a vital role in inducing the differentiation of Tregs and thereby mediates the pro-tumoral immunosuppression of immune cells.<sup>100–103</sup>

We found elevated gene expression of *Cd206* and *Tgf- $\beta$*  both in J774 and BMDM cells that were co-cultured with control cancer cells, compared to macrophage monocultures. However, in case the cancer cells were exposed to either AuNPs or AgNPs and placed in co-culture with the macrophages, the expression of these M2 markers was again lower. The *Chil3* mRNA and protein expressions were also increased in BMDM-cancer cell co-cultures; however, AuNP treatment reduced these mRNA levels significantly. Investigation of these M2-TAM markers provided strong evidence that although the presence of cancer cells triggered the tumor-promoting M2 polarization program of macrophages; nevertheless, metal nanoparticles were capable of disrupting this cellular manipulation by indirectly suppressing the expression of these markers.

The results on mRNA and protein profiles of J774 and BMDM macrophages presented so far clearly indicated that treating cancer cells with AuNPs or AgNPs would significantly modulate the expression profile (various M1- and M2-like TAM marker genes) of macrophages in the close microenvironment of these cancer cells, suggesting that both nanoparticles can efficiently inhibit the tumor-promoting macrophage reprogramming of cancerous cells. Since elevated migratory capacity is a well-known characteristic of TAMs,<sup>104</sup> we investigated this feature of J774 cells in the presence of 4T1 cells and metal nanoparticles. Results of the migration assays indicated that J774 macrophages co-cultured with cancer cells had higher migration capacity, which was successfully reduced upon treatment with AuNPs and AgNPs. Additionally, the protein levels of CCL2 and CCL3,<sup>105,106</sup> chemokines that are inherently involved in the migration and recruitment of macrophages, were higher in J774 cells co-cultured with untreated tumor cells. However, their amount decreased significantly after AuNP and AgNP treatment (although in the case of CCL3, only AgNPs were efficient). Reports revealed that secretion of CCL3 into the TME enhances cancer cell migration and invasion through the CCL3/CCR5 (C-C chemokine receptor type 5) pathway and is associated with poor prognosis in esophageal squamous cell carcinoma.<sup>19,107,108</sup> Also, CCL2 secreted by TAMs triggered MMP9 upregulation and induced the development of invasive cancer phenotypes.<sup>109,110</sup> The CCL3-CCR1 (chemokine receptor-1), as well as the CCL2/CCR2 signaling pathways, are involved in specific macrophage-related events since both CCL2 and CCL3 are key mediators in recruiting monocytes into the TME, inducing their differentiation into immunosuppressive M2-like TAMs, modulating the proportion of M1 and M2 macrophages, and providing antiapoptotic or angiogenic signals.<sup>111,112</sup> Based on our results, it is evident that disruption of this CCL2 and CCL3-mediated vicious circle by metal nanoparticles is a viable and efficient tool to attenuate cell migration in the TME and suppress tumor development and dissemination.



Finally, the assessment of MMP activity revealed that co-culturing J774 macrophages with 4T1 cancer cells increased the overall enzyme activity of MMPs compared to those measured for J774 monocultures. As expected, AuNP and AgNP treatments could again counteract this phenomenon and reduce the total MMP activity of J774-4T1 co-cultures. These results were not surprising since gene expression experiments also revealed that *Mmp9* mRNA levels in J774 and BMDM samples increased when these cells were cultured together with cancer cells; however, upon AuNP and AgNP treatments of 4T1 cells, the expression of *Mmp9* was found to be significantly lower. The *Mmp2* expression showed a similar tendency, and the MMP2 and MMP9 protein levels mirrored the above-presented patterns. The gelatinases MMP9 and MMP2 are expressed and secreted by various cells in the TME, also by TAMs, and they contribute to the degradation of the ECM, but also facilitate the release of cytokines and growth factors, such as TGF- $\beta$ .<sup>113–115</sup> The members of the MMP family are known to digest various ECM and basement membrane components (such as collagen, elastin, and fibronectin) and alter cell-cell and cell-matrix adhesions established by integrin, cadherin, selectin, or other cell adhesion molecules and thereby destroy the histological barriers of tumor cell invasion, leading to metastasis and angiogenesis of solid tumors.<sup>116</sup> It has been shown that E-cadherin, a cell-cell adhesion molecule essential for preserving epithelial structure and tissue homeostasis, is directly targeted by several MMPs, including MMP9.<sup>117,118</sup> Apart from gelatinases, M2 macrophages and TAMs were shown to secrete membrane-bound or soluble MMPs, serine proteases, and cathepsins mainly to decompose the ECM and to help in the formation of tumor-associated blood vessels.<sup>119</sup> This protease activity in the TME leads to a significant remodeling of the environment surrounding cancer cells, and assisted by the loosened cell-matrix adhesions, enhances cancer cell migration.<sup>120</sup> In fact, MMP2 and MMP9 secreted by TAMs augmented the invasiveness and migratory capacity of MCF7 breast cancer cells.<sup>121</sup> The remodeling of the ECM can also influence local immune responses, affecting primarily the infiltration and activity of immune cells within the TME.<sup>122,123</sup> Taken altogether, suppression of the expression and extracellular proteolytic activity of MMPs or other proteases by AgNPs or AuNPs creates a serious hurdle for tumor cell invasion. Based on our findings, we believe that nanoparticles can impair the TAM-secreted MMP-associated ECM degradation and restrain the tumor dissemination supporting functions that were forced upon TAMs by the neighboring cancer cells. We believe that nanoparticle treatment of cancer cells would modify the cancer cell-released signals and thereby less MMPs would be produced by stromal macrophages. In fact, less MMPs would probably also be generated by stromal fibroblasts and by the cancer cells themselves. This all culminates in an overall decrease in extracellular MMP level and activity leading to less ECM degradation. Additionally, since MMPs contribute to the facilitation of cell motility, the mitigation of MMP secretion and activity by AuNPs and AgNPs results in attenuated migratory capacity of TAMs, CAFs and cancer cells, and thereby to a reduced invasiveness.

Overall, both AuNPs and AgNPs produced similar indirect effects on specific macrophage marker expressions. The minor differences in their impacts can be attributed to their distinct characteristics: AgNPs are cytotoxic and induce the formation of large amounts of free radicals, features which may affect their therapeutic applications. On the other hand, AuNPs are considered to be inert, more biocompatible, less toxic than AgNPs, and excellent candidates for radio-sensitization and targeted drug delivery, which properties favor their future clinical utilization.

J774 and BMDM macrophages, despite their different origins, reacted similarly both to co-culturing with 4T1 cells as well as to exposures to nanoparticle-treated tumor cells, implying the translatability of these results to other in vitro and maybe to in vivo settings. Nevertheless, some differences were naturally detected between these cell cultures on the gene or protein expression levels. Such differences are explainable based on the fact that the J774 cell line is derived from a lymphoma-afflicted mouse,<sup>124,125</sup> and these cells could already be in a relatively engaged state compared to the more naive BMDMs, which are isolated directly from the bone marrow. In fact, research indicates that these two types of macrophages respond slightly differently to bacterial presence;<sup>126</sup> therefore, some immune mechanisms could occur differently in them based also on the type and grade of the stimuli.

Our project focuses on the indirect modulatory function of AuNPs and AgNPs exerted on TAMs and on the capacity of these nanomaterials to disrupt the paracrine communication within the TME. We believe that the internalized nanoparticles are capable of modulating directly the expression and secretion profile of 4T1 cancer cells; therefore, the secreted signals sent towards the stromal cells are different than those secreted in the absence of nanoparticles. Among the critical secreted signals, there are presumably cytokines, chemokines, or other soluble factors, or various mRNA or non-coding RNA molecules packaged, for example, in extracellular vesicles, or exosomes. These protein or RNA factors would reach and affect the macrophages in their close vicinity and induce



a certain molecular program in these cells, depending on the signal. Such a cascade of events leads to altered gene expression and functional features and to a slightly different polarization profile of TAMs. Tumor-derived microRNAs (miRNAs) and long non-coding RNAs (lncRNAs) are gaining more and more attention as possible paracrine modulatory molecules in this cellular crosstalk. In fact, a tumor cell-derived exosomal miRNA (miR-138-5p) was shown to inhibit the epigenetic factor lysine demethylase 6B expression and, thereby blocking M1 polarization of macrophages. Colorectal cancer-derived exosomes contained high levels of miR-934, which downregulated the phosphatase and tensin homolog PTEN, activated the PI3K/Akt pathway, and enhanced the M2 polarization of TAMs.<sup>127</sup> Similarly, miR-145, secreted in tumor-derived extracellular vesicles, promoted M2 polarization by inhibiting histone deacetylase 11,<sup>128</sup> and fostering a tumor-supportive communication between macrophages and cancer cells. The lncRNA known as metastasis-associated lung adenocarcinoma transcript-1 (MALAT1) has been shown to enhance global chromatin accessibility and trigger the production of CCL2, thereby driving the recruitment of pro-tumorigenic TAMs.<sup>129</sup> In an *in vivo* breast cancer mouse model, it was found that the lncRNA-SNHG1 affected the polarization of M2 macrophages by increasing the phosphorylation level of STAT6, whereas silencing of lncRNA-SNHG1 in macrophages inhibited the pro-angiogenic and tumorigenic effects associated with these M2-like macrophages.<sup>130</sup> Based on these and other examples, it is plausible that AuNPs and AgNPs disrupt the paracrine communication between cancer and stromal cells, trigger a significant alteration in the composition of cancer cell-secreted molecules, the type and amount of soluble protein factors, or exosome-packaged miRNAs, and lncRNAs would be modified, thereby disturbing the original macrophage reprogramming plan of cancer cells.

Although our results point to the modulatory activity of metal nanoparticles on the paracrine reprogramming of stromal macrophages and support the above-described potential scenario, we are aware of the limitations of the study. We performed *in vitro* co-culture experiments using membrane inserts, where macrophage cells were incubated together with 4T1 cells for 24 or 48 hours. These co-incubation times, according to many published papers, are sufficient to study the effect of tumor cells on macrophage transformation and modulation.<sup>131–135</sup> A disadvantage of such indirect co-culture systems is that the communication between spatially separated cells does not precisely model the cell-cell interactions observed in the *in situ* tissue environment. We are currently examining cancer cell-macrophage interactions by using conditioned media to molecularly dissect and validate which component/s and molecular mechanisms are responsible for the attenuated TAM properties and the reduced tumor-supporting properties in macrophages. Non-coding RNA molecules are in the focus of these investigations. Although the present work utilizes an oversimplified model to study what might be occurring between cancer cells and macrophages, yet these results indicate that in addition to tumor cells and fibroblasts, TAMs may also be good therapeutic targets for metal nanoparticles in future treatment modalities. Although, in recent years, there was a considerable advancement in our understanding of the cellular and systemic effects of nanoparticles, numerous questions still linger about their potential clinical applications. The magnitude and the duration of the nanoparticles' induced effects and their potential toxicity would clearly depend on the administration route and on certain nanoparticle characteristics (size, morphology, surface charge, stabilizing material, functionalization). Based on *in vivo* studies, it appears that a single administration of metal nanoparticles can effectively produce and sustain several anticancer effects, suggesting prolonged actions of nanoparticles *in vivo*; however, regular or continuous application of nanoparticles may also be necessary to maintain their efficacy when longer-lasting effects are required.<sup>23,34,136–138</sup> Given the limitations of their intravenous use, there is an opportunity to explore their therapeutic roles in localized applications, particularly in intra- and peritumoral settings. Particles can be introduced into the TME either in their free-form or embedded within a biocompatible matrix, such as a hydrogel. Similar to brachytherapy, the localization of nanoparticles near the tumor site could enhance the effectiveness of both chemotherapy and radiotherapy. While there are many promising avenues for the clinical application of metal nanoparticles, additional research is essential to accurately assess their biological activity in *in vivo* settings.

## Conclusion

We believe that our study stands out in that it successfully demonstrates the indirect modulatory effect of metal nanoparticles on J774 immortalized and BMDM primary macrophage cells co-cultured with cancer cells. AuNPs and AgNPs could efficiently modulate macrophage-cancer cell interactions and were able to suppress the cancer cell-induced M2-like TAM marker gene expression, cytokine, and protease production, leading to attenuated matrix metalloprotease

activity and diminished migratory capacity of macrophages. Although both nanoparticles successfully counteracted the reprogramming of macrophages imposed by cancer cells, each nanoparticle manifested a somewhat selective efficacy on different markers, and considering the biocompatible nature of AuNPs, these would be preferred for future oncotherapeutic considerations. J774 and BMDMs, despite their different origins, reacted similarly both to co-culturing with 4T1 cells as well as to exposures to nanoparticle-treated tumor cells, which not only validates the findings obtained but also implies that these results are robust enough to be generally expected from other macrophages, eg, also those residing in vivo in the TME, in similar settings. Although this work represents an oversimplified model of what might be occurring between cancer cells and macrophages of a tumor, these results indicate that in addition to tumor cells, TAMs may also be good therapeutic targets for metal nanoparticles in future treatment modalities. The hypothetical mechanism of altering TAM gene expression and function indirectly by metal nanoparticles may lie in the modulation of soluble factors such as cytokines or non-coding RNAs secreted by cancer cells that favor the induction of M1 macrophage polarization; nevertheless, this notion needs to be examined by further experiments.

In conclusion, our results indicate that AuNPs and AgNPs may represent a valuable and exploitable strategy to disrupt tumor–stroma interactions, counterbalance the “brainwashing” of stromal cells and attenuate the supporting role of macrophages in tumor development, thereby opening innovative avenues for future therapeutic utilizations.

## Ethics Statement

All animal-related experiments were performed according to institutional and EU ethical guidelines, equivalent to the Guide for the Care and Use of Laboratory Animals, in the possession an ethical clearance obtained from the institutional review board of the Biological Research Center, then the National Animal Experimentation and Ethics Board (XVI/766/2018).

## Acknowledgments

The project was supported by the OTKA-NKFIH (K142371) and OTKA-NKFIH (PD143320) grants from the National Research, Development, and Innovation Office of the Hungarian Government. Financial support was also provided by the Incubation Competence Centre of the Centre of Excellence for Interdisciplinary Research, Development and Innovation of the University of Szeged (N.I. is the member of Molecular mechanisms of nanoparticle-induced radiosensitization research group). D.I.A. was supported by the NTP-NFTÖ-22-B-0100 and NTP-NFTÖ-21-B-0157 grants of the National Excellence Program of the Ministry of Human Resources. A.R. and N.I. were supported by the János Bolyai Research Fellowship of the Hungarian Academy of Sciences (BO/00384/21/7 for A.R., BO/00351/22/8 for NI), by the New National Excellence Program of the Ministry of Human Capacities of Hungary (ÚNKP-22-5-SZTE-583, ÚNKP-23-5-SZTE-687 for A.R., ÚNKP-23-5-SZTE-680 for N.I.), and by the University Research Scholarship Program of the Ministry for Culture and Innovation from the source of the National Research, Development and Innovation Fund (EKÖP-24-4-SZTE-626 for N.I.). Open access publication was supported by the University of Szeged (grant number: 7667). The graphical abstract was created in Biorender (Gacser, A. (2025) <https://BioRender.com/c28m314>).

## Disclosure

The authors declare that the research was conducted in the absence of any commercial or financial relationships that could be construed as a potential conflict of interest.

## References

1. Classen A, Lloberas J, Celada A. Macrophage activation: classical versus alternative. *Methods mol Biol.* 2009;531:29–43. doi:10.1007/978-1-59745-396-7\_3
2. Shapouri-Moghaddam A, Mohammadian S, Vazini H, et al. Macrophage plasticity, polarization, and function in health and disease. *J Cell Physiol.* 2018;233(9):6425–6440. doi:10.1002/jcp.26429
3. Wang L, Zhang S, Wu H, Rong X, Guo J. M2b macrophage polarization and its roles in diseases. *J Leukoc Biol.* 2019;106(2):345–358. doi:10.1002/JLB.3RU1018-378RR
4. Murray PJ, Allen JE, Biswas SK, et al. Macrophage activation and polarization: nomenclature and experimental guidelines. *Immunity.* 2014;41(1):14–20. doi:10.1016/j.immuni.2014.06.008
5. Gao J, Liang Y, Wang L. Shaping Polarization Of Tumor-Associated Macrophages In Cancer Immunotherapy. *Front Immunol.* 2022;13:888713. doi:10.3389/fimmu.2022.888713

6. Cortez-Retamozo V, Etzrodt M, Newton A, et al. Origins of tumor-associated macrophages and neutrophils. *Proc Natl Acad Sci U S A*. 2012;109(7):2491–2496. doi:10.1073/pnas.1113744109
7. Franklin RA, Liao W, Sarkar A, et al. The cellular and molecular origin of tumor-associated macrophages. *Science*. 2014;344(6186):921–925. doi:10.1126/science.1252510
8. Whiteside TL. The tumor microenvironment and its role in promoting tumor growth. *Oncogene*. 2008;27(45):5904–5912. doi:10.1038/onc.2008.271
9. Martinez FO, Sica A, Mantovani A, Locati M. Macrophage activation and polarization. *FBL*. 2008;13(2):453–461.
10. Pittet MJ, Michielin O, Migliorini D. Clinical relevance of tumour-associated macrophages. *Nat Rev Clin Oncol*. 2022;19(6):402–421. doi:10.1038/s41571-022-00620-6
11. Mantovani A, Allavena P, Marchesi F, Garlanda C. Macrophages as tools and targets in cancer therapy. *Nat Rev Drug Discov*. 2022;21(11):799–820. doi:10.1038/s41573-022-00520-5
12. Wang S, Wang J, Chen Z, et al. Targeting M2-like tumor-associated macrophages is a potential therapeutic approach to overcome antitumor drug resistance. *Npj Precis Oncol*. 2024;8(1):31. doi:10.1038/s41698-024-00522-z
13. Elinav E, Nowarski R, Thaiss CA, Hu B, Jin C, Flavell RA. Inflammation-induced cancer: crosstalk between tumours, immune cells and microorganisms. *Nat Rev Cancer*. 2013;13(11):759–771. doi:10.1038/nrc3611
14. Canli Ö, Nicolas AM, Gupta J, et al. Myeloid Cell-Derived Reactive Oxygen Species Induce Epithelial Mutagenesis. *Cancer Cell*. 2017;32(6):869–883.e5. doi:10.1016/j.ccell.2017.11.004
15. Liu S, Li Q, Chen K, et al. The emerging molecular mechanism of m6A modulators in tumorigenesis and cancer progression. *Biomed Pharmacother*. 2020;127:110098. doi:10.1016/j.biopha.2020.110098
16. Wertheimer T, Zwicky P, Rindlisbacher L, et al. IL-23 stabilizes an effector Treg cell program in the tumor microenvironment. *Nat Immunol*. 2024;25(3):512–524. doi:10.1038/s41590-024-01755-7
17. Li D, Ji H, Niu X, et al. Tumor-associated macrophages secrete CC-chemokine ligand 2 and induce tamoxifen resistance by activating PI3K/Akt/mTOR in breast cancer. *Cancer Sci*. 2020;111(1):47–58. doi:10.1111/cas.14230
18. Chen W, Chen M, Hong L, et al. M2-like tumor-associated macrophage-secreted CCL2 facilitates gallbladder cancer stemness and metastasis. *Exp Hematol Oncol*. 2024;13(1):83. doi:10.1186/s40164-024-00550-2
19. Kodama T, Koma Y, Arai N, et al. CCL3–CCR5 axis contributes to progression of esophageal squamous cell carcinoma by promoting cell migration and invasion via Akt and ERK pathways. *Lab Invest*. 2020;100(9):1140–1157. doi:10.1038/s41374-020-0441-4
20. Li H, Yang B, Huang J, et al. Cyclooxygenase-2 in tumor-associated macrophages promotes breast cancer cell survival by triggering a positive-feedback loop between macrophages and cancer cells. *Oncotarget*. 2015;6(30):29637–29650. doi:10.18632/oncotarget.4936
21. Nakanishi Y, Nakatsuji M, Seno H, et al. COX-2 inhibition alters the phenotype of tumor-associated macrophages from M2 to M1 in ApcMin/+ mouse polyps. *Carcinogenesis*. 2011;32(9):1333–1339. doi:10.1093/carcin/bgr128
22. Zhao T, Zeng J, Xu Y, et al. Chitinase-3 like-protein-1 promotes glioma progression via the NF-κB signaling pathway and tumor microenvironment reprogramming. *Theranostics*. 2022;12(16):6989–7008. doi:10.7150/thno.75069
23. Kovács D, Igaz N, Marton A, et al. Core-shell nanoparticles suppress metastasis and modify the tumour-supportive activity of cancer-associated fibroblasts. *J Nanobiotechnology*. 2020;18(1):18. doi:10.1186/s12951-020-0576-x
24. Valkenburg KC, de Groot AE, Pienta KJ. Targeting the tumour stroma to improve cancer therapy. *Nat Rev Clin Oncol*. 2018;15(6):366–381. doi:10.1038/s41571-018-0007-1
25. Xu M, Zhang T, Xia R, Wei Y, Wei X. Targeting the tumor stroma for cancer therapy. *mol Cancer*. 2022;21(1):208. doi:10.1186/s12943-022-01670-1
26. Wu C, Zhai Y, Ji J, et al. Advances in tumor stroma-based targeted delivery. *Int J Pharm*. 2024;664:124580. doi:10.1016/j.ijpharm.2024.124580
27. Sagnella SM, McCarroll JA, Kavallaris M. Drug delivery: beyond active tumour targeting. *Nanomedicine Nanotechnol Biol Med*. 2014;10(6):1131–1137. doi:10.1016/j.nano.2014.04.012
28. Carreón González JL, García Casillas PE, Chapa González C. Gold Nanoparticles as Drug Carriers: the Role of Silica and PEG as Surface Coatings in Optimizing Drug Loading. *Micromachines*. 2023;14(2). doi:10.3390/mi14020451
29. Jain PK, Huang X, El-Sayed IH, El-Sayed MA. Noble metals on the nanoscale: optical and photothermal properties and some applications in imaging, sensing, biology, and medicine. *Acc Chem Res*. 2008;41(12):1578–1586. doi:10.1021/ar7002804
30. Miranda RR, Sampaio I, Zucolotto V. Exploring silver nanoparticles for cancer therapy and diagnosis. *Colloids Surf B Biointerfaces*. 2022;210:112254. doi:10.1016/j.colsurfb.2021.112254
31. Kaur R, Singh K, Agarwal S, Masih M, Chauhan A, Gautam PK. Silver nanoparticles induces apoptosis of cancer stem cells in head and neck cancer. *Toxicol Reports*. 2024;12:10–17. doi:10.1016/j.toxrep.2023.11.008
32. Selim ME, Hendi AA. Gold nanoparticles induce apoptosis in MCF-7 human breast cancer cells. *Asian Pac J Cancer Prev*. 2012;13(4):1617–1620. doi:10.7314/apjcp.2012.13.4.1617
33. Kovács D, Igaz N, Keskeny C, et al. Silver nanoparticles defeat p53-positive and p53-negative osteosarcoma cells by triggering mitochondrial stress and apoptosis. *Sci Rep*. 2016;6:27902. doi:10.1038/srep27902
34. Brzóska K, Wojewódzka M, Szczygiel M, et al. Silver Nanoparticles Inhibit Metastasis of 4T1 Tumor in Mice after Intragastric but Not Intravenous Administration. *Mater*. 2022;15(11):3837. doi:10.3390/ma15113837
35. Igaz N, Szóke K, Kovács D, et al. Synergistic Radiosensitization by Gold Nanoparticles and the Histone Deacetylase Inhibitor SAHA in 2D and 3D Cancer Cell Cultures. *Nanomaterials*. 2020;10(1). doi:10.3390/nano10010158
36. Yang X, Yang M, Pang B, Vara M, Xia Y. Gold Nanomaterials at Work in Biomedicine. *Chem Rev*. 2015;115(19):10410–10488. doi:10.1021/acs.chemrev.5b00193
37. Soares S, Aires F, Monteiro A, et al. Radiotherapy Metastatic Prostate Cancer Cell Lines Treated with Gold Nanorods Modulate miRNA Signatures. *Int J mol Sci*. 2024;25(5):2754. doi:10.3390/ijms25052754
38. Amaral MN, Nunes D, Fortunato E, et al. Gold nanoparticles for photothermal therapy – influence of experimental conditions on the properties of resulting AuNPs. *J Drug Deliv Sci Technol*. 2024;101:106215. doi:10.1016/j.jddst.2024.106215
39. De Jong WH, Van Der Ven LTM, Sleijffers A, et al. Systemic and immunotoxicity of silver nanoparticles in an intravenous 28 days repeated dose toxicity study in rats. *Biomaterials*. 2013;34(33):8333–8343. doi:10.1016/j.biomaterials.2013.06.048

40. Ma Q, Lim CS. Molecular Activation of NLRP3 Inflammasome by Particles and Crystals: a Continuing Challenge of Immunology and Toxicology. *Annu Rev Pharmacol Toxicol*. 2024;64:417–433. doi:10.1146/ANNUREV-PHARMTOX-031023-125300/CITE/REFWORKS
41. Benetti F, Bregoli L, Olivato I, Sabbioni E. Effects of metal(loid)-based nanomaterials on essential element homeostasis: the central role of nanometallomics for nanotoxicology. *Metallomics*. 2014;6(4):729–747. doi:10.1039/c3mt00167a
42. Báez DF, Gallardo-Toledo E, Oyarzún MP, Araya E, Kogan MJ. The Influence of Size and Chemical Composition of Silver and Gold Nanoparticles on in vivo Toxicity with Potential Applications to Central Nervous System Diseases. *Int J Nanomed*. 2021;16:2187–2201. doi:10.2147/IJN.S260375
43. Chrastina A, Schnitzer JE. Iodine-125 radiolabeling of silver nanoparticles for in vivo SPECT imaging. *Int J Nanomed*. 2010;5:653–659. doi:10.2147/IJN.S11677
44. Liu J, Liu Z, Pang Y, Zhou H. The interaction between nanoparticles and immune system: application in the treatment of inflammatory diseases. *J Nanobiotechnology*. 2022;20(1):127. doi:10.1186/s12951-022-01343-7
45. Reichel D, Tripathi M, Perez JM. Biological Effects of Nanoparticles on Macrophage Polarization in the Tumor Microenvironment. *Nanotheranostics*. 2019;3(1):66–88. doi:10.7150/ntno.30052
46. Bastús NG, Sánchez-Tilló E, Pujals S, et al. Homogeneous Conjugation of Peptides onto Gold Nanoparticles Enhances Macrophage Response. *ACS Nano*. 2009;3(6):1335–1344. doi:10.1021/nm8008273
47. Zazo H, Colino CI, Warzecha KT, et al. Gold Nanocarriers for Macrophage-Targeted Therapy of Human Immunodeficiency Virus. *Macromol Biosci*. 2017;17(3). doi:10.1002/mabi.201600359
48. Yen H-J, Hsu S-H, Tsai C-L. Cytotoxicity and immunological response of gold and silver nanoparticles of different sizes. *Small*. 2009;5(13):1553–1561. doi:10.1002/sml.200900126
49. Nishanth RP, Jyotsna RG, Schlager JJ, Hussain SM, Reddanna P. Inflammatory responses of RAW 264.7 macrophages upon exposure to nanoparticles: role of ROS-NFκB signaling pathway. *Nanotoxicology*. 2011;5(4):502–516. doi:10.3109/17435390.2010.541604
50. Sarkar S, Leo BF, Carranza C, et al. Modulation of Human Macrophage Responses to Mycobacterium tuberculosis by Silver Nanoparticles of Different Size and Surface Modification. *PLoS One*. 2015;10(11):e0143077. doi:10.1371/journal.pone.0143077
51. Pal R, Chakraborty B, Nath A, et al. Noble metal nanoparticle-induced oxidative stress modulates tumor associated macrophages (TAMs) from an M2 to M1 phenotype: an in vitro approach. *Int Immunopharmacol*. 2016;38:332–341. doi:10.1016/j.intimp.2016.06.006
52. Hao Y, Duan F, Dong X, et al. Gold Nanoparticle Inhibits the Tumor-Associated Macrophage M2 Polarization by Inhibiting m 6 A Methylation-Dependent ATG5/Autophagy in Prostate Cancer. *Anal Cell Pathol*. 2025;2025(1):6648632. doi:10.1155/ancp/6648632
53. Wan Y, Guo Z, Jiang X, et al. Quasi-spherical silver nanoparticles: aqueous synthesis and size control by the seed-mediated Lee–Meisel method. *J Colloid Interface Sci*. 2013;394:263–268. doi:10.1016/j.jcis.2012.12.037
54. Deng Z, Ma S, Zhou H, et al. Tyrosine phosphatase SHP-2 mediates C-type lectin receptor–induced activation of the kinase Syk and anti-fungal TH17 responses. *Nat Immunol*. 2015;16(6):642–652. doi:10.1038/ni.3155
55. Bourgeois C, Majer O, Frohner I, Kuchler K. In vitro systems for studying the interaction of fungal pathogens with primary cells from the mammalian innate immune system. *Methods mol Biol*. 2009;470:125–139. doi:10.1007/978-1-59745-204-5\_11
56. Ghosn EEB, Cassado AA, Govoni GR, et al. Two physically, functionally, and developmentally distinct peritoneal macrophage subsets. *Proc Natl Acad Sci*. 2010;107(6):2568–2573. doi:10.1073/pnas.0915000107
57. Yashiro T, Nakano S, Nomura K, Uchida Y, Kasakura K, Nishiyama C. A transcription factor PU.1 is critical for Ccl22 gene expression in dendritic cells and macrophages. *Sci Rep*. 2019;9(1):1161. doi:10.1038/s41598-018-37894-9
58. Röhrle N, Knott MML, Anz D. CCL22 Signaling in the Tumor Environment. *Adv Exp Med Biol*. 2020;1231:79–96. doi:10.1007/978-3-030-36667-4\_8
59. Chen J, Zhao D, Zhang L, et al. Tumor-associated macrophage (TAM)-derived CCL22 induces FAK addiction in esophageal squamous cell carcinoma (ESCC). *Cell mol Immunol*. 2022;19(9):1054–1066. doi:10.1038/s41423-022-00903-z
60. Gschwandtner M, Derler R, Midwood KS. More Than Just Attractive: how CCL2 Influences Myeloid Cell Behavior Beyond Chemotaxis. *Front Immunol*. 2019;10:2759. doi:10.3389/fimmu.2019.02759
61. Granot Z, Henke E, Comen EA, King TA, Norton L, Benezra R. Tumor entrained neutrophils inhibit seeding in the premetastatic lung. *Cancer Cell*. 2011;20(3):300–314. doi:10.1016/j.ccr.2011.08.012
62. Nie W, Yu T, Sang Y, Gao X. Tumor-promoting effect of IL-23 in mammary cancer mediated by infiltration of M2 macrophages and neutrophils in tumor microenvironment. *Biochem Biophys Res Commun*. 2017;482(4):1400–1406. doi:10.1016/j.bbrc.2016.12.048
63. Subhadarshani S, Yusuf N, Elmets CA. IL-23 and the Tumor Microenvironment. *Adv Exp Med Biol*. 2021;1290:89–98. doi:10.1007/978-3-030-55617-4\_6
64. Parameswaran N, Patial S. Tumor necrosis factor-α signaling in macrophages. *Crit Rev Eukaryot Gene Expr*. 2010;20(2):87–103. doi:10.1615/criteveukargeneexpr.v20.i2.10
65. Lejeune FJ, Liénard D, Matter M, Rüegg C. Efficiency of recombinant human TNF in human cancer therapy. *Cancer Immun*. 2006;6:6.
66. Qiao Y, Huang X, Nimmagadda S, et al. A robust approach to enhance tumor-selective accumulation of nanoparticles. *Oncotarget*. 2011;2(1–2):59–68. doi:10.18632/oncotarget.227
67. Mercogliano MF, Bruni S, Mauro F, Elizalde PV, Schillaci R. Harnessing Tumor Necrosis Factor Alpha to Achieve Effective Cancer Immunotherapy. *Cancers*. 2021;13(3). doi:10.3390/cancers13030564
68. Balkwill F. Tumour necrosis factor and cancer. *Nat Rev Cancer*. 2009;9(5):361–371. doi:10.1038/nrc2628
69. Cruceriu D, Baldasici O, Balacescu O, Berindan-Neagoe I. The dual role of tumor necrosis factor-α (TNF-α) in breast cancer: molecular insights and therapeutic approaches. *Cell Oncol*. 2020;43(1):1–18. doi:10.1007/s13402-019-00489-1
70. Rubio MF, Werbach S, Cafferata EGA, et al. TNF-α enhances estrogen-induced cell proliferation of estrogen-dependent breast tumor cells through a complex containing nuclear factor-kappa B. *Oncogene*. 2006;25(9):1367–1377. doi:10.1038/sj.onc.1209176
71. Rivas MA, Carnevale RP, Proietti CJ, et al. TNF alpha acting on TNFR1 promotes breast cancer growth via p42/P44 MAPK, JNK, Akt and NF-kappa B-dependent pathways. *Exp Cell Res*. 2008;314(3):509–529. doi:10.1016/j.yexcr.2007.10.005
72. Qiao Y, He H, Jonsson P, Sinha I, Zhao C, Dahlman-Wright K. AP-1 Is a Key Regulator of Proinflammatory Cytokine TNFα-mediated Triple-negative Breast Cancer Progression\*. *J Biol Chem*. 2016;291(10):5068–5079. doi:10.1074/jbc.M115.702571



73. Pileczki V, Braicu C, Gherman CD, Berindan-Neagoe I. TNF- $\alpha$  Gene Knockout in Triple Negative Breast Cancer Cell Line Induces Apoptosis. *Int J mol Sci.* **2013**;14(1):411–420. doi:10.3390/ijms14010411
74. Baumgarten SC, Frasor J. Minireview: inflammation: an instigator of more aggressive estrogen receptor (ER) positive breast cancers. *mol Endocrinol.* **2012**;26(3):360–371. doi:10.1210/me.2011-1302
75. Donato NJ, Klostergaard J. Distinct stress and cell destruction pathways are engaged by TNF and ceramide during apoptosis of MCF-7 cells. *Exp Cell Res.* **2004**;294(2):523–533. doi:10.1016/j.yexcr.2003.11.021
76. Simstein R, Burrow M, Parker A, Weldon C, Beckman B. Apoptosis, chemoresistance, and breast cancer: insights from the MCF-7 cell model system. *Exp Biol Med.* **2003**;228(9):995–1003. doi:10.1177/153537020322800903
77. Mortara L, Balza E, Sassi F, et al. Therapy-induced antitumor vaccination by targeting tumor necrosis factor alpha to tumor vessels in combination with melphalan. *Eur J Immunol.* **2007**;37(12):3381–3392. doi:10.1002/eji.200737450
78. Gamble JR, Harlan JM, Klebanoff SJ, Vadas MA. Stimulation of the adherence of neutrophils to umbilical vein endothelium by human recombinant tumor necrosis factor. *Proc Natl Acad Sci U S A.* **1985**;82(24):8667–8671. doi:10.1073/pnas.82.24.8667
79. Neumann B, Machleidt T, Lifka A, et al. Crucial role of 55-kilodalton TNF receptor in TNF-induced adhesion molecule expression and leukocyte organ infiltration. *J Immunol.* **1996**;156(4):1587–1593. doi:10.4049/jimmunol.156.4.1587
80. Kamada H, Tsutsumi Y, Yamamoto Y, et al. Antitumor activity of tumor necrosis factor- $\alpha$  conjugated with polyvinylpyrrolidone on solid tumors in mice. *Cancer Res.* **2000**;60(22):6416–6420.
81. Watanabe N, Niitsu Y, Umeno H, et al. Toxic effect of tumor necrosis factor on tumor vasculature in mice. *Cancer Res.* **1988**;48(8):2179–2183.
82. Rodríguez D, Silvera R, Carrio R, et al. Tumor microenvironment profoundly modifies functional status of macrophages: peritoneal and tumor-associated macrophages are two very different subpopulations. *Cell Immunol.* **2013**;283(1–2):51–60. doi:10.1016/j.cellimm.2013.06.008
83. Perrotta C, Cervia D, Di Renzo I, et al. Nitric Oxide Generated by Tumor-Associated Macrophages Is Responsible for Cancer Resistance to Cisplatin and Correlated With Syntaxin 4 and Acid Sphingomyelinase Inhibition. *Front Immunol.* **2018**;9:1186. doi:10.3389/fimmu.2018.01186
84. Ridnour LA, Dhanapal S, Hoos M, et al. Nitric oxide-mediated regulation of  $\beta$ -amyloid clearance via alterations of MMP-9/TIMP-1. *J Neurochem.* **2012**;123(5):736–749. doi:10.1111/jnc.12028
85. Ridnour LA, Windhausen AN, Isenberg JS, et al. Nitric oxide regulates matrix metalloproteinase-9 activity by guanylyl-cyclase-dependent and -independent pathways. *Proc Natl Acad Sci.* **2007**;104(43):16898–16903. doi:10.1073/pnas.0702761104
86. Liu B, Qu L, Yan S. Cyclooxygenase-2 promotes tumor growth and suppresses tumor immunity. *Cancer Cell Int.* **2015**;15:106. doi:10.1186/s12935-015-0260-7
87. Kalinski P. Regulation of immune responses by prostaglandin E2. *J Immunol.* **2012**;188(1):21–28. doi:10.4049/jimmunol.1101029
88. Somasundaram V, Ridnour LA, Cheng RY, et al. Systemic Nos2 Depletion and Cox inhibition limits TNBC disease progression and alters lymphoid cell spatial orientation and density. *Redox Biol.* **2022**;58:102529. doi:10.1016/j.redox.2022.102529
89. Basudhar D, Glynn SA, Greer M, et al. Coexpression of NOS2 and COX2 accelerates tumor growth and reduces survival in estrogen receptor-negative breast cancer. *Proc Natl Acad Sci.* **2017**;114(49):13030–13035. doi:10.1073/pnas.1709119114
90. Allavena P, Chieppa M, Bianchi G, et al. Engagement of the mannose receptor by tumoral mucins activates an immune suppressive phenotype in human tumor-associated macrophages. *Clin Dev Immunol.* **2010**;2010:547179. doi:10.1155/2010/547179
91. Bobrie A, Massol O, Ramos J, et al. Association of CD206 Protein Expression with Immune Infiltration and Prognosis in Patients with Triple-Negative Breast Cancer. *Cancers.* **2022**;14(19):4829. doi:10.3390/cancers14194829
92. Heng Y, Zhu X, Lin H, et al. CD206+ tumor-associated macrophages interact with CD4+ tumor-infiltrating lymphocytes and predict adverse patient outcome in human laryngeal squamous cell carcinoma. *J Transl Med.* **2023**;21(1):167. doi:10.1186/s12967-023-03910-4
93. Haque ASMR, Moriyama M, Kubota K, et al. CD206(+) tumor-associated macrophages promote proliferation and invasion in oral squamous cell carcinoma via EGF production. *Sci Rep.* **2019**;9(1):14611. doi:10.1038/s41598-019-51149-1
94. Mao Z, Han Y, Li Y, Bai L. CD206 accelerates hepatocellular carcinoma progression by regulating the tumour immune microenvironment and increasing M2-type polarisation of tumour-associated macrophages and inflammation factor expression. *Discov Oncol.* **2024**;15(1):439. doi:10.1007/s12672-024-01309-1
95. Kang Q, Li L, Pang Y, Zhu W, Meng L. An update on Ym1 and its immunoregulatory role in diseases. *Front Immunol.* **2022**;13:891220. doi:10.3389/fimmu.2022.891220
96. Bastea LI, Liou G-Y, Pandey V, et al. Pomalidomide Alters Pancreatic Macrophage Populations to Generate an Immune-Responsive Environment at Precancerous and Cancerous Lesions. *Cancer Res.* **2019**;79(7):1535–1548. doi:10.1158/0008-5472.CAN-18-1153
97. Fleming Martinez AK, Döppler HR, Bastea LI, Edenfield BH, Liou G-Y, Storz P. Ym1(+) macrophages orchestrate fibrosis, lesion growth, and progression during development of murine pancreatic cancer. *iScience.* **2022**;25(5):104327. doi:10.1016/j.isci.2022.104327
98. Liou G-Y, Bastea L, Fleming A, et al. The Presence of Interleukin-13 at Pancreatic ADM/PanIN Lesions Alters Macrophage Populations and Mediates Pancreatic Tumorigenesis. *Cell Rep.* **2017**;19(7):1322–1333. doi:10.1016/j.celrep.2017.04.052
99. Wu F, Weigel KJ, Zhou H, Wang X-J. Paradoxical roles of TGF- $\beta$  signaling in suppressing and promoting squamous cell carcinoma. *Acta Biochim Biophys Sin.* **2018**;50(1):98–105. doi:10.1093/abbs/gmx127
100. Chen W, Jin W, Hardegen N, et al. Conversion of peripheral CD4+CD25- naive T cells to CD4+CD25+ regulatory T cells by TGF- $\beta$  induction of transcription factor Foxp3. *J Exp Med.* **2003**;198(12):1875–1886. doi:10.1084/jem.20030152
101. Ouyang W, Beckett O, Ma Q, Li MO. Transforming growth factor-beta signaling curbs thymic negative selection promoting regulatory T cell development. *Immunity.* **2010**;32(5):642–653. doi:10.1016/j.immuni.2010.04.012
102. Strauss L, Bergmann C, Szczepanski M, Gooding W, Johnson JT, Whiteside TL. A unique subset of CD4+CD25highFoxp3+ T cells secreting interleukin-10 and transforming growth factor-beta1 mediates suppression in the tumor microenvironment. *Clin Cancer Res.* **2007**;13(15 Pt 1):4345–4354. doi:10.1158/1078-0432.CCR-07-0472
103. Chen M-L, Pittet MJ, Gorelik L, et al. Regulatory T cells suppress tumor-specific CD8 T cell cytotoxicity through TGF- $\beta$  signals in vivo. *Proc Natl Acad Sci U S A.* **2005**;102(2):419–424. doi:10.1073/pnas.0408197102
104. Chen X, Yang M, Yin J, et al. Tumor-associated macrophages promote epithelial-mesenchymal transition and the cancer stem cell properties in triple-negative breast cancer through CCL2/AKT/ $\beta$ -catenin signaling. *Cell Commun Signal.* **2022**;20(1):92. doi:10.1186/s12964-022-00888-2
105. Lin Y, Xu J, Lan H. Tumor-associated macrophages in tumor metastasis: biological roles and clinical therapeutic applications. *J Hematol Oncol.* **2019**;12(1):76. doi:10.1186/s13045-019-0760-3



106. Qin R, Ren W, Ya G, et al. Role of chemokines in the crosstalk between tumor and tumor-associated macrophages. *Clin Exp Med.* **2023**;23(5):1359–1373. doi:10.1007/s10238-022-00888-z
107. Ross JL, Chen Z, Herting CJ, et al. Platelet-derived growth factor beta is a potent inflammatory driver in paediatric high-grade glioma. *Brain.* **2021**;144(1):53–69. doi:10.1093/brain/awaa382
108. Eum HH, Kwon M, Ryu D, et al. Tumor-promoting macrophages prevail in malignant ascites of advanced gastric cancer. *Exp mol Med.* **2020**;52(12):1976–1988. doi:10.1038/s12276-020-00538-y
109. Lee S, Lee E, Ko E, et al. Tumor-associated macrophages secrete CCL2 and induce the invasive phenotype of human breast epithelial cells through upregulation of ERO1- $\alpha$  and MMP-9. *Cancer Lett.* **2018**;437:25–34. doi:10.1016/j.canlet.2018.08.025
110. An J, Xue Y, Long M, Zhang G, Zhang J, Su H. Targeting CCR2 with its antagonist suppresses viability, motility and invasion by downregulating MMP-9 expression in non-small cell lung cancer cells. *Oncotarget.* **2017**;8(24):39230–39240. doi:10.18632/oncotarget.16837
111. Sica A, Saccani A, Bottazzi B, et al. Defective expression of the monocyte chemotactic protein-1 receptor CCR2 in macrophages associated with human ovarian carcinoma. *J Immunol.* **2000**;164(2):733–738. doi:10.4049/jimmunol.164.2.733
112. Sunakawa Y, Stremtizer S, Cao S, et al. Association of variants in genes encoding for macrophage-related functions with clinical outcome in patients with locoregional gastric cancer. *Ann Oncol off J Eur Soc Med Oncol.* **2015**;26(2):332–339. doi:10.1093/annonc/mdl542
113. Jiang H, Li H. Prognostic values of tumoral MMP2 and MMP9 overexpression in breast cancer: a systematic review and meta-analysis. *BMC Cancer.* **2021**;21(1):149. doi:10.1186/s12885-021-07860-2
114. Dofara SG, Chang S-L, Diorio C. Gene Polymorphisms and Circulating Levels of MMP-2 and MMP-9: a Review of Their Role in Breast Cancer Risk. *Anticancer Res.* **2020**;40(7):3619–3631. doi:10.21873/anticancer.14351
115. Song Z, Wang J, Su Q, Luan M, Chen X, Xu X. The role of MMP-2 and MMP-9 in the metastasis and development of hypopharyngeal carcinoma. *Braz J Otorhinolaryngol.* **2021**;87(5):521–528. doi:10.1016/j.bjorl.2019.10.009
116. Kessenbrock K, Plaks V, Werb Z. Matrix metalloproteinases: regulators of the tumor microenvironment. *Cell.* **2010**;141(1):52–67. doi:10.1016/j.cell.2010.03.015
117. Augoff K, Hryniewicz-Jankowska A, Tabola R, Stach K. MMP9: a Tough Target for Targeted Therapy for Cancer. *Cancers.* **2022**;14(7):1847. doi:10.3390/cancers14071847
118. Cowden Dahl KD, Symowicz J, Ning Y, et al. Matrix metalloproteinase 9 is a mediator of epidermal growth factor-dependent e-cadherin loss in ovarian carcinoma cells. *Cancer Res.* **2008**;68(12):4606–4613. doi:10.1158/0008-5472.CAN-07-5046
119. De Palma M, Bizziato D, Petrova TV. Microenvironmental regulation of tumour angiogenesis. *Nat Rev Cancer.* **2017**;17(8):457–474. doi:10.1038/nrc.2017.51
120. Gonzalez-Avila G, Sommer B, Mendoza-Posada DA, Ramos C, Garcia-Hernandez AA, Falfan-Valencia R. Matrix metalloproteinases participation in the metastatic process and their diagnostic and therapeutic applications in cancer. *Crit Rev Oncol Hematol.* **2019**;137:57–83. doi:10.1016/j.critrevonc.2019.02.010
121. Hagemann T, Wilson J, Kulbe H, et al. Macrophages induce invasiveness of epithelial cancer cells via NF-kappa B and JNK. *J Immunol.* **2005**;175(2):1197–1205. doi:10.4049/jimmunol.175.2.1197
122. McQuibban GA, Gong JH, Tam EM, McCulloch CA, Clark-Lewis I, Overall CM. Inflammation dampened by gelatinase A cleavage of monocyte chemoattractant protein-3. *Science.* **2000**;289(5482):1202–1206. doi:10.1126/science.289.5482.1202
123. Sheu BC, Hsu SM, Ho HN, Lien HC, Huang SC, Lin RH. A novel role of metalloproteinase in cancer-mediated immunosuppression. *Cancer Res.* **2001**;61(1):237–242.
124. Hirst JW, CM JGG, Cohn M. Characterization of a BALB/c Myeloma Library. *J Immunol.* **1971**;107(3):926–927. doi:10.4049/jimmunol.107.3.926.c
125. Schwarzbaum S, Diamond B. The J744.2 cell line presents antigen in an I region restricted manner. *J Immunol.* **1983**;131(2):674–677.
126. Andreu N, Phelan J, de Sessions PF, Cliff JM, Clark TG, Hibberd ML. Primary macrophages and J774 cells respond differently to infection with Mycobacterium tuberculosis. *Sci Rep.* **2017**;7(1):42225. doi:10.1038/srep42225
127. Zhao S, Mi Y, Guan B, et al. Tumor-derived exosomal miR-934 induces macrophage M2 polarization to promote liver metastasis of colorectal cancer. *J Hematol Oncol.* **2020**;13(1):156. doi:10.1186/s13045-020-00991-2
128. Shinohara H, Kuranaga Y, Kumazaki M, et al. Regulated Polarization of Tumor-Associated Macrophages by miR-145 via Colorectal Cancer-Derived Extracellular Vesicles. *J Immunol.* **2017**;199(4):1505–1515. doi:10.4049/jimmunol.1700167
129. Martinez-Terroba E, Plasek-Hegde LM, Chiotakakos I, et al. Overexpression of Malat1 drives metastasis through inflammatory reprogramming of the tumor microenvironment. *Sci Immunol.* **2024**;9(96):eadh5462. doi:10.1126/sciimmunol.adh5462
130. Zong S, Dai W, Guo X, Wang K. LncRNA-SNHG1 promotes macrophage M2-like polarization and contributes to breast cancer growth and metastasis. *Aging.* **2021**;13(19):23169–23181. doi:10.18632/aging.203609
131. Dehai C, Bo P, Qiang T, et al. Enhanced invasion of lung adenocarcinoma cells after co-culture with THP-1-derived macrophages via the induction of EMT by IL-6. *Immunol Lett.* **2014**;160(1):1–10. doi:10.1016/j.imlet.2014.03.004
132. Paduch R, Klatka M, Pieniędz P, Wertel I, Pawłowska A, Klatka J. Reciprocal Interactions of Human Monocytes and Cancer Cells in Co-Cultures In Vitro. *Curr Issues mol Biol.* **2024**;46(7):6836–6852. doi:10.3390/cimb46070408
133. Sun W, Li S, Tang G, et al. HHLA2 deficiency inhibits non-small cell lung cancer progression and THP-1 macrophage M2 polarization. *Cancer Med.* **2021**;10(15):5256–5269. doi:10.1002/cam4.4081
134. Park JV, Chandra R, Cai L, et al. Tumor Cells Modulate Macrophage Phenotype in a Novel In Vitro Co-Culture Model of the NSCLC Tumor Microenvironment. *J Thorac Oncol.* **2022**;17(10):1178–1191. doi:10.1016/j.jtho.2022.06.011
135. Zhang Q, Tsui Y-M, Zhang VX, et al. Reciprocal interactions between malignant cells and macrophages enhance cancer stemness and M2 polarization in HBV-associated hepatocellular carcinoma. *Theranostics.* **2024**;14(2):892–910. doi:10.7150/thno.87962
136. Zhang X-D, Wu H-Y, Wu D, et al. Toxicologic effects of gold nanoparticles in vivo by different administration routes. *Int J Nanomed.* **2010**;5:771–781. doi:10.2147/IJN.S8428
137. Yang L, Kuang H, Zhang W, Aguilar ZP, Wei H, Xu H. Comparisons of the biodistribution and toxicological examinations after repeated intravenous administration of silver and gold nanoparticles in mice. *Sci Rep.* **2017**;7(1):3303. doi:10.1038/s41598-017-03015-1
138. Rageh MM, El-Gebaly RH, Afifi MM. Antitumor activity of silver nanoparticles in Ehrlich carcinoma-bearing mice. *Nauryn Schmiedebergs Arch Pharmacol.* **2018**;391(12):1421–1430. doi:10.1007/s00210-018-1558-5

## International Journal of Nanomedicine

### Publish your work in this journal

The International Journal of Nanomedicine is an international, peer-reviewed journal focusing on the application of nanotechnology in diagnostics, therapeutics, and drug delivery systems throughout the biomedical field. This journal is indexed on PubMed Central, MedLine, CAS, SciSearch®, Current Contents®/Clinical Medicine, Journal Citation Reports/Science Edition, EMBase, Scopus and the Elsevier Bibliographic databases. The manuscript management system is completely online and includes a very quick and fair peer-review system, which is all easy to use. Visit <http://www.dovepress.com/testimonials.php> to read real quotes from published authors.

Submit your manuscript here: <https://www.dovepress.com/international-journal-of-nanomedicine-journal>

**Dovepress**  
Taylor & Francis Group